FEASIBILITY OF LOW-COST PRETREATMENT METHODS OF PRODUCED WATER IN THE PERMIAN BASIN

A Thesis

by

DAMIR KAISHENTAYEV

Submitted to the Graduate and Professional School of
Texas A&M University
in partial fulfillment of the requirements for the degree of

MASTER OF SCIENCE

Chair of Committee,	Berna Hascakir
Committee Members,	David Schechter
	Yuefeng Sun
Head of Department,	Jeff Spath

December 2021

Major Subject: Petroleum Engineering

ABSTRACT

With low prices for petroleum and the rising demand for energy sources, most petroleum companies are trying to find ways to make existing technologies more efficient. Since renewable sources have not established themselves as sufficient means to meet energy requests yet, the world is concentrating on unconventional hydrocarbon reservoirs. Hydraulic fracturing, which is an essential part of the current well stimulation process in unconventional fields, requires large amounts of freshwater. At the same time produced water, coming from underground during petroleum production, is considered to be one of the biggest challenges to increase the productivity of wells. To mitigate the scarcity of freshwater and disposal of contaminated produced water, operators are actively investing in technologies that can be used to economically turn wastewater into clean water.

In this study, the efficacy of the coagulation-flocculation–sedimentation (CFS) process was investigated on 14 produced water samples collected from the Permian basin. First, the samples were characterized in terms of pH, total suspended solids (TSS), total dissolved solids (TDS), zeta potential (ZP), turbidity, organic matter presence, and ion concentrations. Then, a jar test was used to pretreat these wastewater samples in a laboratory. Varying doses of alum and ferric sulfate were tested in the coagulation process. In the flocculation process cationic starch and polyamine were tested with a dose of 20 mg/L. After the jar test pH, TSS, TDS, ZP, and turbidity of samples were measured again. The optimum dose of the coagulants was determined based on the maximum TSS removal.

All measured values of the parameters at optimum coagulant doses were analyzed by using Pearson correlation.

Produced water characterization results indicated that the samples are high in TDS and dissolved Na^+ and Cl^- ions are the main reason for that. Zeta potential analyses showed that TSS in the wastewaters are mainly negatively charged. The most TSS reduction of 86% on average was achieved by addition of ferric sulfate as a coagulant. In some wells, the addition of cationic starch as a flocculant showed 10% on average reduction in TDS. Pearson correlation revealed some positive correlations between TDS and ZP, Ca^+ and Mg^+ ions. On the other hand, the negative correlations were determined for TSS and depth, Li and depth, ferric sulfate optimal dose and ZP, and TDS and pH.

ACKNOWLEDGEMENTS

First and foremost, I want to thank my academic adviser, Dr. Berna Hascakir, for her unwavering support of my MS studies and research, as well as her patience, inspiration, passion, and vast expertise. Her advice was invaluable during the research and writing of my thesis.

Apart from my adviser, I'd like to express my gratitude to the members of my thesis committee: Dr. David Schechter and Dr. Yuefeng Sun, for their support and insightful remarks.

I'd like to thank my Heavy Oil, Oil shale, Oil sands, and Carbonate Analysis and Recovery Methods (HOCAM) Group colleagues Lifu Zhang, Alex Cortes and Tanya Mathews for fascinating conversations, long hours spent working together, and all the fun we've had over the last two years. I am very thankful to Karen Chen for her advice and motivation on how to stay focused on my studies and be productive as a student.

Last but not least, I'd like to express my gratitude to my family for supporting me throughout my life.

CONTRIBUTORS AND FUNDING SOURCES

Contributors

This work was supervised by a thesis committee consisting of Dr. Berna Hascakir (advisor and committee chair) and Dr. David Schechter of the Department of Petroleum Engineering and Dr. Yuefeng Sun of the Department of Geology and Geophysics.

The ICP-MS analyses depicted in Chapter III were conducted in part by Luz Romero of the Department of Geology and Geophysics.

All other work conducted for the thesis was completed by the student independently.

Funding Sources

Graduate study was supported by a fellowship from Texas A&M University and a thesis research fellowship from the Berg-Hughes Center for Petroleum & Sedimentary Systems.

This work was also made possible by Bolashak Scholarship under the Center for International Programs, the Republic of Kazakhstan.

NOMENCLATURE

CFS	Coagulation-flocculation-sedimentation
EOR	Enhanced oil recovery
IC	Ion chromatography
ICP-MS	Inductively coupled plasma mass spectrometry
NM	Northern Midland
OD	Optimal dose
PW	Produced water
RO	Reverse osmosis
SM	Southern Midland
TDS	Total dissolved solids
TGA/DSC	Thermo-gravimetric analysis/ Differential scanning calorimetry
TOC	Total organic carbon
TSS	Total suspended solids
XRD	X-ray diffraction
ZP	Zeta potential

TABLE OF CONTENTS

Page

LIST OF FIGURES

Page

LIST OF TABLES

Page

CHAPTER I

INTRODUCTION AND LITERATURE REVIEW

From the 20th century, oil and gas have often been regarded as the world's primary energy source (Environmental & Energy Study Institute, 2021). Since then, they have been one of the main driving forces behind technological progress. Nevertheless, nowadays, most developed countries are trying to switch to environmentally friendly renewable energies like solar, wind, geothermal, etc. However, in 2017, fossil fuels met 80% of global energy consumption, with renewables accounting for just 18% (Ren21: Global Overview, 2019). According to US EIA (2019), by 2050, the need for energy will be increased by 50%, with oil and gas still covering at least 49%. To keep up with rising energy requests, the US has started actively extracting hydrocarbons from unconventional reservoirs. As a result, the country overcame Russia as the world's biggest natural gas producer in 2011 and surpassed Saudi Arabia as the world's top oil producer in 2018 (US EIA 2019). This technological achievement was possible mainly due to advances in horizontal drilling and hydraulic fracturing stimulations (Smith & Ziane, 2012).

Since unconventional petroleum deposits have very poor permeability, feasible economic extraction of fuels requires the implementation of multistage fracturing (Pei et al. 2020). Nowadays, this technology might use up to 14 million gallons of fresh water per well (Platt et al. 2011). Slickwater fracturing, especially in unconventional reservoirs, is a very popular stimulation approach across the petroleum industry. This method can provide more complex fracture geometry than conventional crosslinked fluids due to the lower

viscosity and higher injection rates (Mayerhofer et al. 1997). However, as a flipside, this technique requires a large volume of clean make-up water (Palisch et al. 2010).

When preparing fracking fluid, it is critical to take into account the compatibility of constituents. Seawater, for example, has a high concentration of various salts, pathogens, and suspended particles (Buck 1974). If such substances are used as part of fracturing fluid without being removed, they will induce scaling, tube corrosion, and formation damage (Nasr-El-Din 2003). Freshwater, on the other hand, has been utilized as the primary make-up fluid without complex treatment for decades because it contains a few pollutants. However, this practice has one tremendous drawback. According to Shiklomanov (2000), just 0.0065% of the world's water sources may be deemed readily available as freshwater in the form of lakes and rivers. He adds that the situation becomes even more alarming when we include unequal distribution of potable water, rising industrial demand, and increasing water pollution. Many scientists claim that global temperatures will rise, causing the spread of arid areas and the scarcity of drinking water (Lancon & Hascakir, 2018). As a result, two-thirds of the world's population may suffer fresh water shortages by 2025 if present consumption rates continue (Brown et al. 2019). These circumstances are having a massive impact on all industries, including oil and gas. As a result, numerous petroleum organizations across the globe are working with governments to devise procedures to decrease the consumption of freshwater. Methods that allow the use produced water (PW), brackish reservoirs, and wastewater from facilities for industry needs, are gaining a lot of interest (Ng et al. 2018). However, the

quality and consistency of these sources vary greatly, necessitating careful treatment and processing steps.

In the treatment of industrial effluent, many stand alone and combined physical, biological and chemical technologies are employed. These methods include membrane filtration, thermal, biological aerated filters, hydrocyclones, gas flotation, evaporation ponds, adsorption, and several other methods. The main drawback of all these methods is that they are not economically feasible or environmentally adverse or both. Waite (2010) asserts, for small communities with limited freshwater resources, desalination techniques may provide enough potable water. However, the author adds, reverse osmosis (RO), a popular method for removing salt from water, requires much energy, making it challenging to implement as a sustainable technology for industrial needs. Moreover, because of the released brine, desalination plants may potentially contaminate the environment. Also, these membrane-based processes are not suited to treat high TDS waters and are not persistent to prevailing contaminants, such as free oil and suspended solids (Hassinger et al. 1994).

It should be noted, there are no specific requirements for the quality of treated water to be reused as fracturing fluid; it depends on the geology and geochemistry of the formation and the expected properties (Rodriguez et al. 2020). Nevertheless, we can say, the closer the quality of the treated water to freshwater the better. Typically, most operator companies consider TSS, turbidity, TDS, hardness, organic matter, and heavy metals as the main contaminants (Igunnu & Chen, 2012). At the same time, Liden et al. (2019) claim TDS is not a critical issue as long as the ions (e.g., Ba, B, Ca, Fe, and Sr) that might induce

scaling or negatively influence the solution chemistry are kept to appropriate levels. For example, in 2013, Halliburton successfully reused recycled water with TDS of 285,000 ppm in the Permian basin and helped operators to save $500,000 (Halliburton 2013) on fracturing operations. In another case, zirconium-crosslinked fluids have been reported to work with PW from Bakken formation that had TDS over 300,000 ppm (Kakadjian et al. 2013).

On the other hand, unlike TDS, the removal of TSS has always been critical requirement (Zhang & Hascakir, 2020). Solids come from a variety of places, including formation particles and compounds from the injection and production facilities. If these suspended particulates are not removed before use, clogging and bridging of the pore space in the formation may occur quickly and severely which can significantly reduce the fracture conductivity (Oort et al. 1993; Ali & Hascakir, 2018). According to Ye et al. (2013), the two general methods that are used to reduce TSS include absorption and straining. The authors say absorption is a physicochemical process that relies on chemical and electrostatic forces; straining, on the other hand, is based on filters that have smaller diameters than contaminants. Among a number of different technologies, because of its simplicity of use, high effectiveness, and cheap cost, coagulation-flocculation-sedimentation (CFS) is one of the most favored methods in initial water treatment (Altaher et al. 2011). Furthermore, it uses less energy than other common techniques (Tatsi et al. 2003).

CFS may utilize organic, inorganic, or a mixture of these chemicals. The most commonly used organic chemicals are polymers. They are utilized extensively in various

phases of drilling, completion, workover, and production of oil and gas. Polymers can be classified into two main groups: natural and synthetic (Akash et al. 2014). Natural polymers originate in nature, and synthetic polymers are chemically reacted monomers. The primary benefits of synthetic polymers over natural ones are higher thermal stability and contamination resistance. Nevertheless, natural polymers, according to Macczak et al. (2020), have sparked a lot of attention due to their advantages over synthetic and inorganic agents. Synthetic chemicals are considered to be more toxic and harmful for people and for the environment (Bolto & Gregoryba, 2007). Organic alternatives have a number of benefits, including biodegradability, non-toxicity, the ability to undergo a variety of chemical modifications, and broad availability.

All inorganic chemicals used in water treating plants could be categorized into four main types by application: lime is used for precipitation softening, coagulants and flocculants are used to remove TSS and colloidal solids, powdered activated carbon is used for taste and odor, and disinfectants are used to remove bacteria (Subhash et al. 2016). As coagulants and flocculants, most companies prefer to use salts of aluminum and/or iron due to their low cost and accessibility (Hassan & Mousa, 2017). Nearly 75% of all aluminum produced is still in use today, making it endlessly recyclable and long-lasting material (Aluminum association, 2021). Likewise, iron is the cheapest and the most abundant metal, which makes it a very popular reagent for water treatment methods (JLab, 2021).

When salts of aluminum and iron are introduced to water during the coagulation process, they produce a range of metal hydrolysis products. Resulted cationic compounds

absorb negatively charged particles and neutralize their charge (Jiang 2015 as cited in Malik 2018). Flocculation, on the other hand, is a process in which destabilized particles are linked together by hydrogen bonding or Van der Waals forces to form larger flocs, which are then entrapped, and more particulate is removed by settling down (Ratnayaka et al. 2009). It should be emphasized that the flocculation stage may or may not be required, depending on the efficacy of the coagulation process and treatment expectations. In the majority of cases, these chemicals are chosen based on the initial water quality, process equipment, and treatment objectives which are closely related to the financial capability of the operating companies.

Some fluids injected into a well may get back to the surface during the production stage (Vidic et al. 2013). These waters, an article in National Geographic states, compared to naturally occurring "produced water" from formations, mostly resemble injected fluids and are referred to as "the flowback water." On the other hand, the article claims, PW has more common characteristics with formation water as high TDS and a lower Total organic carbon (TOC) concentration. Oil and grease, as well as dissolved organic components, are part of TOC, which is a common contaminant in the flowback water (Khalilpour 2014). The free-water knock-out tank, three-phase separator, and gravity settling tank are used to remove free oil from water, whereas dissolved air flotation tank may remove dispersed oil from water. The majority of dissolved oil may be removed by air-stripping technique (Fang & Lin 1988). Although it is not explicit how to distinguish PW from the flowback water, some experts believe that if the production time exceeds one month, it may be classified as PW (Gregory et al. 2011; Esmaeilirad et al. 2016).

In general, as hydrocarbon production rises, so does the quantity of produced byproducts. The vast amount of PW is considered to be one of the most significant issues in the oil and gas industry that restricts the petroleum production rate (Reynolds 2003). PW is basically a byproduct of all hydrocarbon fields (Scanlon et al. 2017). As a field matures, the issue will become more prevalent. As a result, the PW flow rate rises throughout the operating time until the field becomes uneconomic to exploit anymore.

Water production has long been a routine procedure in most conventional oil fields, and most of it could be reinjected back to the formation to boost hydrocarbon output. However, it is not a possibility for unconventional reservoirs owing to very poor permeability (Yong et al. 2012). As a consequence, tons of PW have been injected into shallow saltwater disposal wells, creating problems such as micro-scale earthquakes and surface water pollution (Kondash et al. 2016). Unfortunately, there is no official statistics that can fully represent the true situation regarding PW management. Though some US states keep careful track of generated water, most of them don't have much information on how the water is handled since there is no federal data-collecting effort (Clark & Veil, 2007). Nevertheless, using correlations and available data from 32 states, Veil (2020) presented an approximate amount of PW in the US for 2007, 2012, and 2017. He claims approximately 21 billion barrels of PW were generated in 2007. At the same time, in another report by Guerra et al. (2011), the authors suggested approximately 7 billion barrels of PW had been recovered each year which is 3 times less than calculated by Veil. In this study approximations from Veil's report were used. Because he presented more detailed information and his reports were referred to by many other researchers and

government agencies across the industry. As of 2017, Veil says 24.4 billion barrels of PW were generated. Contribution of each state presented in Table 1. It can be seen that Texas, California, and Oklahoma alone were accountable for 62% of all PW in the country.

Table 1: Produced water volumes due to oil and gas production in the US in 2017 and respective rankings and the contribution of each state

Ranking	**US State**	**PW volume, *10^6 bbl**	**Share of a state compared to total US produced water**
1	Texas	9,895	41%
2	California	3,134	13%
3	Oklahoma	2,844	12%
4	Wyoming	1,705	7%
5	Kansas	1,205	5%
6	Louisiana	998	4%
7	New Mexico	879	4%
8	Alaska	828	3%
9	Federal offshore	575	2%
10	North Dakota	505	2%

Moreover, he described how these waters were managed by each period of time (Table 2). As can be seen, in 2017, 82% of total PW was injected underground: 44% for enhanced oil recovery (EOR) and 38% for non-commercial disposal wells. A further 10% was pumped into offsite commercial disposal facilities, which are third-party companies that charge a fee to accept PW. Those companies treat and process the water in a number of different ways, but in most cases, they end up injecting into disposal wells at commercial sites. A total of 5.5% of the waste was released into the surface waters. Less

than 1% of PW was evaporated from onsite ponds and pits, as well as in some commercial disposal sites. Within the oil and gas sector, 1.4% was reused for uses other than injection for EOR. This includes recycling PW for use as drilling and fracking fluids for new wells in the same fields. 1.3% of the oil and gas waste was utilized in non-oil and gas uses such as irrigation and dust suppression (Veil 2017).

Table 2: Produced water management methods in 2012 and 2017 in the US

Category	**2012**	**2017**
Injection for EOR, %	45.1	43.6
Injection for disposal, %	38.9	38
Surface discharge, %	5.4	5.5
Evaporation, %	3.4	0.4
Offsite Commercial disposal, %	6.7	9.9
Beneficial reuse, %	0.6	2.7

In many places in the US, the fresh water supply may be cut by a third in as little as 50 years (National Geographic, 2021). As a result, potable water sources are becoming more limited and costly each year. On the other hand, as mentioned above, petroleum companies struggle to keep with the vast volume of contaminated water from wells. In the map (Figure 1), provided by Scanlon et al. (2020), it is clearly shown that the amount of PW in the country, overall, is much larger than the amount of water needed for fracturing. This fact is particularly pertinent to the Permian basin, where the ratio exceeds 2.5.

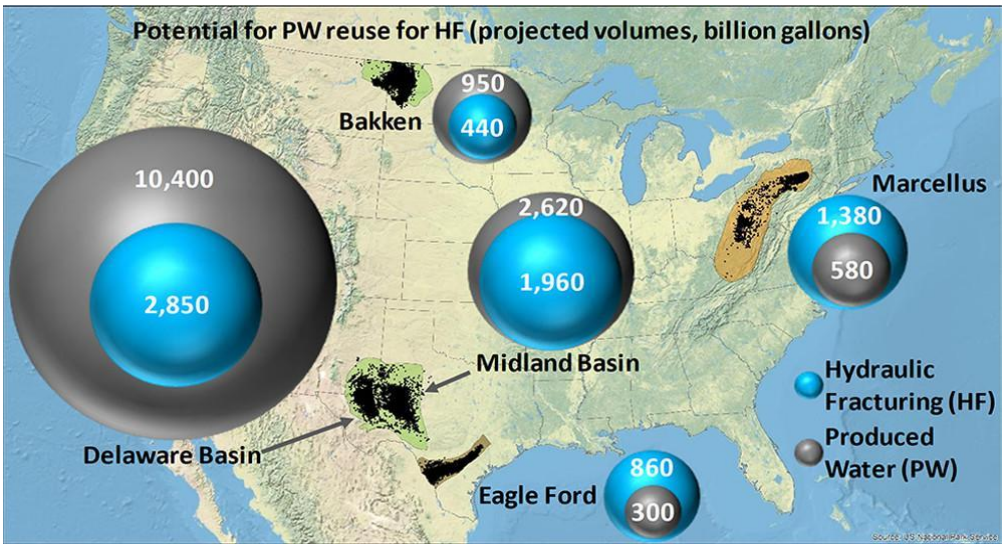

Figure 1: Projected Hydraulic Fracturing (HF, given with blue bubbles) water use and Produced Water (PW, given with grey bubbles) volumes based on the future well inventories (Scanlon et al.2020)

Thus, this research investigates the efficacy of CFS as a pretreatment method of the PW. The main focus of this study was concentrated on reducing TSS of recovered water using coagulants and flocculants. Also, a statistical model was used to determine the correlation between PW parameters and the optimal dose of the chosen coagulants. By determining the relationship between these parameters, it is possible to create more complex models that will allow predicting the optimal dose for different basins.

CHAPTER II

MATERIALS AND METHODS

Materials

A significant part of hydrocarbon production in the US comes from Texas, which produced 43% of the nation's crude oil and 26% of the nation's natural gas in 2020 (EIA 2021). The most prolific spot in Texas is the Permian basin which accounted for 63% of the state's total oil production (US EIA, 2019). The Wolfcamp and Bone Spring formations alone have confirmed technically recoverable quantities of 50 billion barrels of oil and over 300 trillion cubic feet of natural gas (Enverus, 2021). Consequently, Texas is believed to be generating more than 35% of all PW in the US (Guerra et al. 2011). As the Permian basin is the most active oil-producing area in the country, it is crucial to manage PW in this region properly (Krauss 2019). Because, in five years, the basin might be producing 32 million barrels of PW per day, putting even more pressure on local oil companies (Reese 2020).

In the scope of this work, 14 PW samples were studied from various areas of the Permian basin: five from the Northern Midland (NM), five from the Southern Midland (SM), and four from Delaware. The study area map along with the well locations is given in Figure 2.

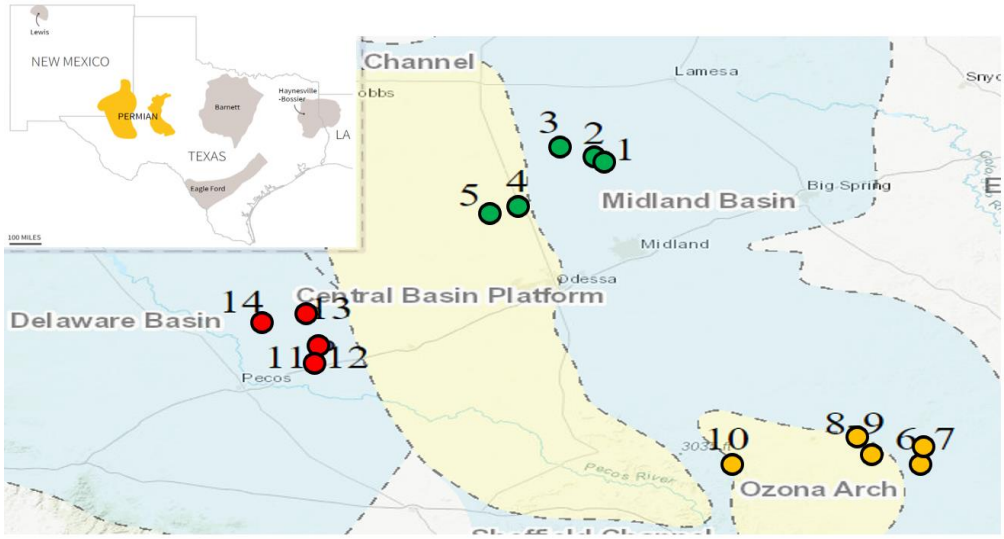

Figure 2: Study area - the well locations in the Permian basin where the samples were collected (adapted from University Lands website)

Every well in this study is oil-producing, horizontal, and hydraulically fractured. Moreover, since all selected wells have been producing oil for more than one month at the time of water sample collection, all collected samples were assumed to be PW. The wells were chosen from the University Lands territory based on the relative high water cut, the prospective location for future fracturing, and the possibility to gather the samples. They are produced from varying formations that have different geologic properties (Table 3). First three wells are from the North Midland sub-basin and they are all located in Spraberry formation (Figure 2 and Table 3). This formation is characterized by turbidite sandstones and laminated siltstones that are interbedded with organic-rich mudrocks (Bureau of Economic Geology UT, 2021). Both fourth and fifth wells are also from North Midland, but their formations are Mississippian and Devonian, respectively. Mississippian formation includes a basal, carbonate succession and an overlying fine grained siliciclastic

mudrock succession (Bureau of Economic Geology UT, 2021). On the other hand, Devonian formation mostly comprised of chert and carbonates (Montgomery, 1998).

Bryndzia et al. (2019) examined 87 core samples of Wolfcamp shale from the Delaware sub-basin and concluded that quartz, K-feldspar and plagioclase are the dominant minerals (~70 wt.%). Clay minerals are muscovite (~2%), illite-smectite (I-S; ~15 wt.%) and chlorite (2 wt.%). The carbonates are mainly calcite and dolomite and typically represent ~10 wt.% of the whole rock. In some samples, dolomite may constitute up to ~80 wt.% of the whole rock.

Table 3: Depth and geological formation information for each well of the Study area given in Figure 2

Well number	Depth, ft	Formation
1	9,422	Spraberry
2	9,818	Spraberry
3	9,641	Spraberry
4	11,573	Mississippian
5	10,851	Devonian
6	6,682	Wolfcamp
7	6,304	Wolfcamp
8	7,192	Wolfcamp
9	6,694	Wolfcamp
10	7,876	Spraberry
11	11,188	Wolfcamp
12	11,668	Wolfcamp
13	12,340	Wolfcamp
14	11,533	Bonespring

Table 4 summarizes the initial water/oil ratio and oil production rate, oil production period, and depth of wells in the study area. As can be seen, the deepest wells are located in the Delaware sub-basin, and these wells have the highest initial WOR

compared to Midland sub-basins. This correlates with Scanlon et al.'s (2019) findings, which claim the amount of PW in the western part of the Permian exceeds the eastern section two times. However, high initial oil production rates are not representative of the current capabilities of each sub-basin. Because Delaware produces about 60% of total Permian oil output annually and Midland produces about 40% (EIA 2021; Global Data Energy 2020).

Table 4: Average Initial water/oil ratio, total oil production time, and depth of the wells grouped by sub-basins

Sub-basin names	Initial oil production rate, bbl/d	Initial WOR*	Production duration, month	Depth, ft
North Midland	1,295	2.72	24	9,729
South Midland	820	4.18	23	6,949
Delaware	1,013	4.25	17	11,463

WOR* - water oil ratio

In Figure 3 the pictures of the initial PW samples can be seen. From the picture it is obvious that samples collected from the Delaware Sub-Basin (Sample 11, 12, 13, and 14 in Figure 3) are much more transparent than the samples from the North and South Sub-Basins.

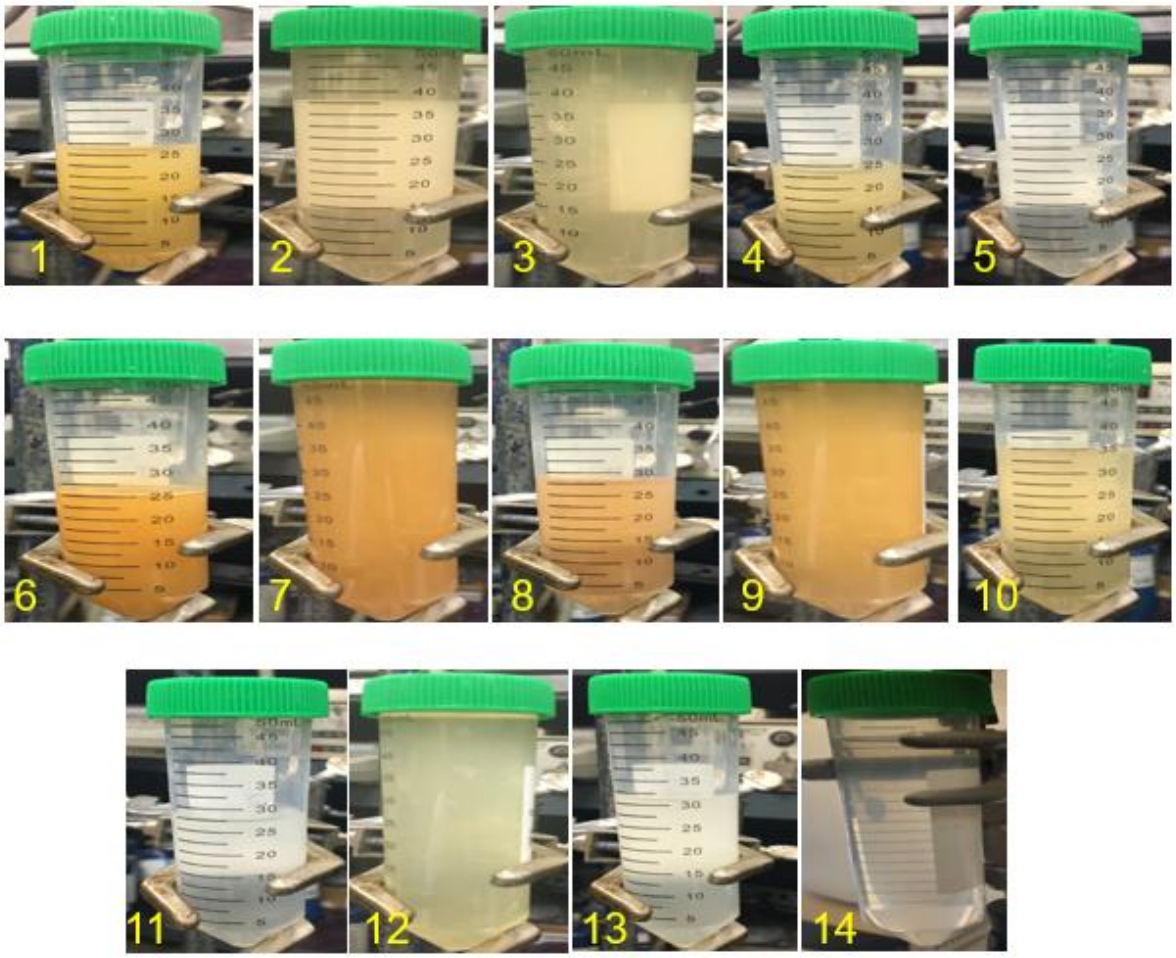

Figure 3: Pictures of the initial produced water samples with well numbers indicated in yellow (Samples given in the first row are from the Northern Midland, in the second row are from the Southern Midland, and in the third row are from the Delaware sub-basin)

For the pretreatment of these wastewaters collected from 14 different wells, the coagulation/flocculation/sedimentation (CFS) method was selected. Because CFS, as described in the previous section, is the most preferred way to reduce TSS. Alum ($Al_2(SO_4)_3*18H_2O$) and Ferric sulfate ($Fe_2(SO_4)_3$) were chosen as coagulants. Cationic starch and Polyamine (Bis(hexamethylene)triamine) were used as organic flocculants in this study. Alum is typically an odorless white crystalline solid. This chemical is the most

commonly used coagulant in the petroleum sector, and it often does not need any extra supplements (Brandt et al. 2016). Ferric sulfate is yellow water-soluble salt. Compared to alum, it has some advantages. For example, the flock particles of ferric hydroxides have a much higher density than alum flocks and are more easily removed by sedimentation (Pal 2017). However, ferric sulfate can stain equipment and is difficult to dissolve, and its solution is corrosive. Both reagents are three valence-based compounds. When colloids are negatively charged, charge neutralization is more effective when the cation has a higher value (Hardy 1900). We must keep in mind that overdose may cause charge reversal and particle restabilization; thus, precise coagulant dosage is required for charge neutralization (Aften & Zhang, 2016). Moreover, inadequate coagulation may result in excessive coagulant residuals in treated water, as well as particle precipitation after pretreatment (Sahu & Chaudhari, 2013).

Cationic starch and Polyamine were used as organic flocculants in this study. Starch is a member of polysaccharides, and its repeating unit is glucose, having a carbohydrate monomer composition of $C_6H_{12}O_6$. It is typically delivered as a white powder. The chosen polyamine is aliphatic polyamine with formula $C_{12}H_{29}N_3$. They are delivered as brown and milky wet powder.

Methods

A Phipps & Bird PB jar tester was used to mimic the coagulation, flocculation, and sedimentation (CFS) process at laboratory conditions (Figure 4). This jar test apparatus contains six beacons that mix water and reagents, allowing it to simulate real plant

conditions to some degree. Alum and ferric sulfate were tested as coagulants and cationic starch and polyamine were tested as flocculants. To estimate the optimal dose of coagulants, six distinct dosages of coagulants (55, 150, 300, 420, 580, and 700 mg/L) were added to the beakers at the coagulation step. These doses were based on economic assumptions. The minimum dose 55 mg/L was used because less than this concentration did not give any visible results. On the other hand, the maximum dose of 700 mg/L was selected because more concentration would be too expensive to use as a part of pretreatment. Because most water treating companies in the US spend on average $0.2-8.5 per 1 barrel of PW (Dahm & Chapman, 2014). But high costs typically refer to tertiary treatment with complex technologies and high-quality results. That's why the threshold of $0.5 for chemicals was used since other expenses like labor, energy and so on must be also considered. But in the case of flocculants the price was not taken into account. Cationic starch is very expensive to be used as a chemical in real treatment facilities. The prices of the chosen chemicals are indicated in Table 5.

Table 5: Prices for the coagulants and flocculants used in the study (Sigma-Aldrich, 2020)

	Laboratory Chemicals			**Industry Chemicals**
	mass, g	price, $US	Price per 1kg, $US	Price per 1kg, $US
Alum	500	240	480	3.7
$Fe_2(SO_4)_3$	250	40	160	NA
Cationic starch	0.25	196	784,000	NA
Polyamine	210	40	190	NA

The jar tester was set to 300 rpm for 1 minute for the coagulation stage and 40 rpm for 30 minutes during the flocculation step. Finally, it was turned off for 30 minutes in the sedimentation phase without being rotated. After the determination of the optimum coagulant doses, the jar tester was used to determine the performance of flocculants. For these experiments, after the addition of optimum coagulant doses to the beakers just before the coagulation step, the jar tester was set to 300 rpm for 1 minute for the coagulation stage. Then, just before the flocculation step 20 mg/L dose of either cationic starch or poly amine was added to the beakers and the jar tester was set to 40 rpm for 30 minutes during the flocculation step. Finally, it was turned off for 30 minutes in the sedimentation phase without being rotated.

Figure 4: Picture of a Jar test apparatus (Courtesy of DalcoInternational)

Total suspended solids (TSS) do not settle or separate using traditional physical techniques due to the nature of the colloidal solution (Farajnezhad & Gharbani, 2012). Thus, the optimum doses of the coagulants were decided based on the removal efficiency of the total suspended solids (TSS) in wastewater samples. The quantity of TSS was determined by filtering 100 mL of wastewater samples through a 1.5 μm paper filter and drying it in an oven at 104°C (EPA 160.2). The used filters were cleansed with DI water to ensure that no residual TDS weight influenced the measurement precision.

Apart from the TSS parameter, both initial and treated water samples were analyzed for pH, TDS, and turbidity to estimate the performance of the CFS process.

When considering possible changes in the coagulation process, it is important to adopt an aggregated view of treatment objectives, as well as to evaluate coagulation as a multiple input process that can be fine-tuned by adjusting major parameters (Budd et al. 2004 as cited in Sahu & Chaudhari, 2013). The pH of fracturing fluid is very important when considering certain chemical additives as they might not be compatible. A high pH value generally results in a strong tendency of scaling, and a low pH value leads to high corrosiveness (Renpu 2011). For example, if the pH of water exceeds 9.5, then Ca and Mg may precipitate and cause damage to the formation (Tariq et al. 2019). That's why it is common practice to regulate pH by adding certain chemicals if indicators are not preferable. The pH of each sample was measured using Oakton PC700 Meter. This equipment can detect up to 0.01 change in pH.

Zeta potential determination is an important characterization method for estimating the surface charge of suspended particles that may be used to better understand

better the physical stability of nanosuspensions (Jiang et al. 2009). Due to the electrostatic repulsion of individual particles, a high positive or negative zeta potential of nanocrystals indicates excellent physical stability (Joseph & Singhvi, 2019). The main purpose of the coagulation step is to reduce the absolute value of repulsion and allow particles to stick together. NanoBrook ZetaPALS Potential Analyzer was used to examine the ZP of the samples. Due to high TDS, the water samples were diluted to 1:100 and filtered using a 1.5 μm paper filter.

Turbidity is a measurement of a liquid's relative clarity. When a light is shone through a water, it is a measurement of the quantity of light dispersed by material in the water (USGS: turbidity & water, 2021). Typically, clay, silt, extremely small inorganic and organic particles, and dissolved colored organic compounds contribute to the turbidity. This indicator is one of the most common in water treatment facilities since it can be measured very quickly without complex procedures. The AquaFast 4500 was used to determine turbidity without any filtration or dilution.

Ion chromatography (IC Thermo Scientific) and inductively coupled plasma mass spectrometry (ICP-MS Element XR) were used to examine the elemental composition of PW samples. Quantities of Mo, Cd, Sb, Pb, U, Al, Si, P, S, Cr, Mn, Fe, Co, Ni, Cu, Ti, Zn, B, Sr, Ba, Na, Ca, K, NH_4, Mg, As, Li, Cl, Br, F, SO_4, NO_3 were identified during the analyses. 1:1000 dilution of filtered PW sample was made in ICP-MS analysis after making each sample 2% nitric acid (HNO3), and a 1:100 dilution was made in IC analysis according to the operating requirement of equipment. To protect the mentioned equipment, I filtered the samples using a 0.45 μm paper filter before taking measurements.

While n-Alkanes are the predominant organic compounds of PW, there are also other constituents like organic acids, benzene, toluene, ethylbenzene, xylene (BTEX), and polycyclic aromatic hydrocarbon present (Ojagh et al. 2020). The amount of dissolved and dispersed organics in PW is hazardous to the environment, and concentrations, sometimes, maybe high in some oil fields (Veil et al. 2004). NETZSCH Thermogravimetric analysis/ Differential scanning calorimetry (TGA/DSC) was used to determine organic matter present in the samples. The main principle of TGA, thermogravimetric analysis, is to measure a sample's mass as it is heated or cooled. In this study, the PW samples were heated up to 600°C with nitrogen and oxygen injection at a constant rate of 10°C/min. When the temperature is above 100°C, water from samples starts to evaporate. After exceeding 350-400°C, organic matter decomposes to form ash, heat, light, water, carbon dioxide, and some other gases (Chapin et al. 2011). As a result, the weight between 100 to 400°C corresponds to the organic content of the samples.

The TDS of the samples were determined using the Oakton PC700 meter. Equipment designed to quantify TDS cannot measure it directly since their working principle relies on measuring electric conductivity and translating it into TDS (Walton 1989). As a result, the readings highly rely on temperature. Water samples were diluted 1:10 with DI water to get more reliable indications owing to the high concentration of salts in all samples and instrument sensitivity.

To check the mineralogy of the sample residues, the total solids in each produced water sample were analyzed with an X-Ray diffractometer (Bruker SMART APEX). 100

ml of each wastewater sample was evaporated in an oven at 105°C which contains both TDS and TSS.

As the final step, experimental results were used in a statistical model called Pearson coefficients. The goal was to determine the connection between the different characteristics of the samples and the optimal dose of chosen chemicals.

The correlation coefficient is a metric that indicates the degree to which two variables' movements are linked. The Pearson correlation coefficient, which is the most often used correlation coefficient, is used to quantify the linear connection between two variables (StatisticsSolutions, 2021). This correlation, however, may not always be an appropriate measure of dependency in a non-linear connection (KentState University library, 2021). This method may have a range of values from -1 to 1. A perfect negative correlation is represented by a correlation of -1, whereas a perfect positive correlation is represented by a correlation of 1. There is no connection between the two variables if the value is zero.

A correlation between variables does not always imply that a change in one variable causes a change in the values of the other. Causation, on the other hand, denotes that one event occurs as a consequence of the occurrence of the other, i.e., the two occurrences have a causal connection. The distinction between the two kinds of connections is theoretically straightforward: one action or event may cause another or it can correlate with another. In reality, however, proving cause and effect remains more challenging than showing correlation.

CHAPTER III

EXPERIMENTAL RESULTS AND DISCUSSIONS

Initial produced water characterization

Table 6 summarizes the initial produced water characterization based on average Total suspended solids (TSS), Total dissolved solids (TDS), Zeta potential, Turbidity and pH measurement results given for each sub-basin. Results for each well are given in Appendix C in Table 10.

Table 6: Average pH, total suspended solids (TSS), turbidity, and zeta potential (ZP) values of the samples by sub-basins

Sub-basin	pH	ZP, mV	TSS, mg/L	Turbidity, NTU	TDS, ppm
North Midland	6.91	-14,6	130	266	120,800
South Midland	6.54	-18	389	204	116,300
Delaware	7.36	-28	41	51	47,750

The TGA analysis was conducted to determine the presence of dissolved organic matters in the water samples. It shows weight loss during heating up process, and at around 100°C, the weight loss corresponds to water amount. The TGA results for all 14 samples were similar. Figure 5 shows as an example the TGA graph of Well 5, and as we can see, there was no change in mass when the temperature exceeded 400°C (Burger et al., 1985). The rest TGA results can be found in Appendix B with Figures 36-48. If there were any organics in the sample, at a high temperature, they would have decomposed and caused some weight loss as in the pyrolysis process. But, as can be

seen, there was no weight decrease. This means there is no substantial colloidal organic matter in the PW samples. The low concentration of organics correlates with other studies that state produced water tends to have a very few organic matter (Maguire-Boyle & Barron, 2014). However, since this method uses only a small portion of the water sample, actual indicators might differ from these measurements.

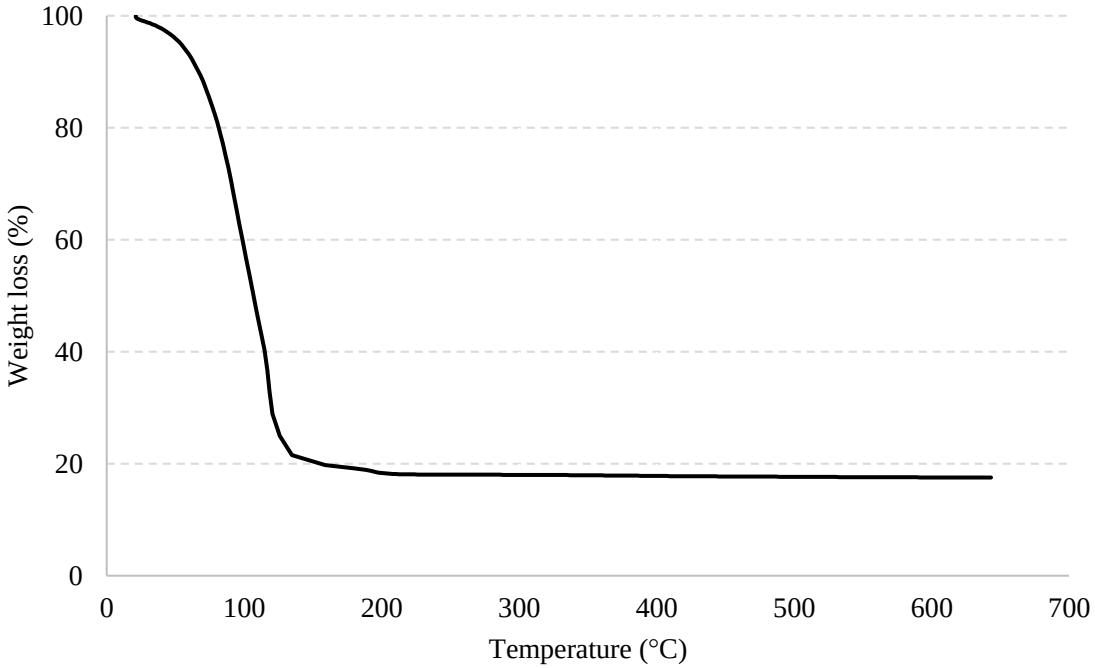

Figure 5: TGA graph example of Well 5 and the other graphs for every well can be found in Appendix B

Total dissolved solids include any inorganic minerals which are in dissolved condition. The TDS components of produced water consists of mainly Na and Cl ions. TDS measurements showed the highest TDS in Well 10 with 153,000 ppm, and the least amount was determined in Well 13 with 41,500 ppm. From Figure 6 it is obvious that TDS

in the Delaware region is much less than in the Midland parts. This might be caused by the dissolution of minerals in meteoric waters in deeper formations (Chaudhary et al. 2016). According to Saller & Stueber (2018), only the upper Permian deposited large quantities of halite in the Permian basin. As a result, both extremely saline fluids that precipitated halite and waters that dissolved halite must have dissolved salts from those shallower stratigraphic intervals. The studies done by Bryndzia et al. (2019) correlates with measurements of this study. They suggested in the Delaware sub-basin high TDS water is mainly coming from shallow regions close to Ochoan evaporites and Salado salts. On the other hand, deep wells with high WOR (>4.5) produced low TDS (<50,000 ppm) waters. Because those waters originated as a result of diagenesis of smectite into illite producing low salinity meteoric water.

XRD analyses was conducted to determine the mineralogy of reject from the water samples. Figure 7 represents the results for Well 1 and the rest results are in Appendix A in Figures 23 to 35. As can be seen, the XRD of residue indicated an abundance of NaCl. NaCl, because of its highly structured crystals, might have suppressed traces of other elements (Zhang & Hascakir, 2018). As a result, XRD was not very helpful in determining the nature of the remaining substances.

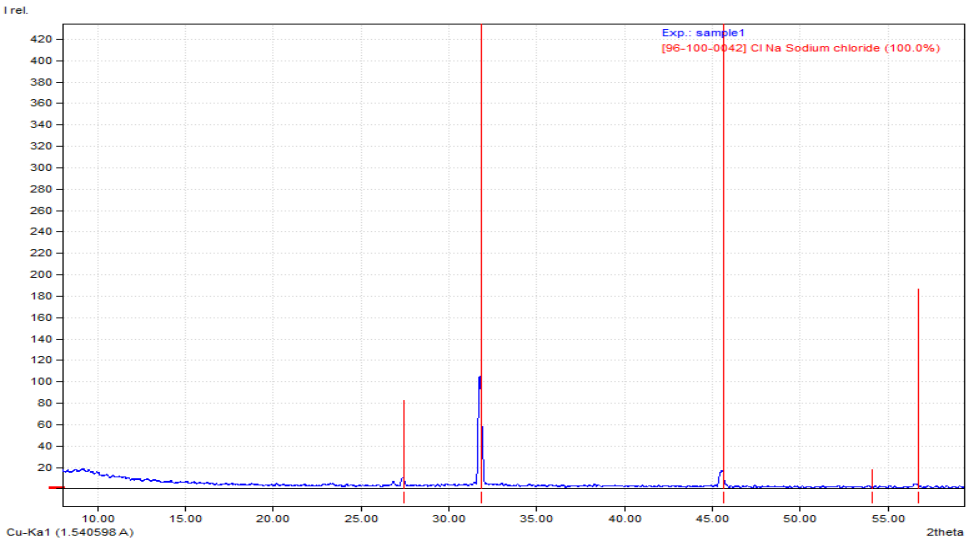

Figure 6: XRD analyses example of residues from Well 1 (the rest of the graphs for every well can be found in Appendix A)

To learn the ion concentration in water samples and elemental composition, ion chromatography and ICP-MS analyses were conducted, respectively. Ion chromatography and ICP-MS results also showed a high concentration of Na^+ and Cl^- ions. According to measurements, all wells have more than 90% NaCl minerals. In the Delaware basin, the amount of SO_4^- ions almost two times higher than in the other two sub-basins.

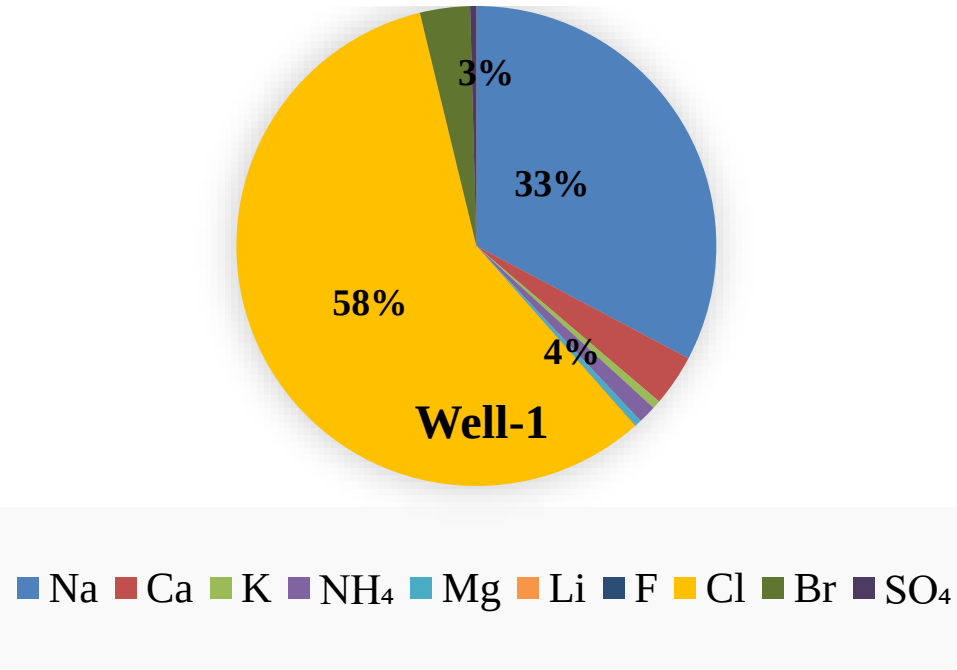

Figure 7: An example of the element composition of the PW sample from Well 1 using Ion chromatography as an example and the rest of the graphs for every well can be found in Appendix D

ICP-MS results also correspond with ion chromatography and X-Ray results, telling NaCl is the most abandoned constituent (Table 7). Though TDS is lower in the Delaware basin, Ba and SO_4 ions are in higher concentrations. This makes it more complicated to use PW without proper treatment because those ions are very susceptible to scaling problems.

Table 7: Concentration intervals of different ions obtained by ICP-MS for each sub-basin

Sub-basin	Concentration (C), ppm	Elements
South Midland	C<10	Mo, Cd, Sb, Pb, U, P, Cr, Mn, Co, Ni, Cu, As, Ba
	10<C<100	Ti, Li
	100<C<1,000	Al, Si, Fe, Zn, B, SO4, Mg, K, S
	1000<C<10,000	Ca, Sr, NH4, Br
	C>10,000	Na, Cl
North Midland	C<10	Mo, Cd, Sb, Pb, U, P, Cr, Mn, Co, Ni, Cu, As
	10<C<100	Ti, Li, Ba
	100<C<1,000	Al, Si, Fe, Zn, B, SO4, Mg, K, NH4, Br
	1000<C<10,000	Ca, Sr, S
	C>10,000	Na, Cl
Delaware	C<10	Mo, Cd, Sb, Pb, U, P, Cr, Mn, Co, Ni, Cu, As
	10<C<100	Ti, Li
	100<C<1,000	Al, Si, Fe, Mg, B, Sr, K, NH4, Br, Ca
	1000<C<10,000	Ba, SO4, S, Zn
	C>10,000	Na, Cl

Figure 8 represents ion distribution when the most common Na, Cl, and Ca ions are excluded. As can be seen in both Midland sub-basins Br, Sr, Mg and NH_4 were second most common ions. On the other hand, in the Delaware sub-basin Ba, Zn, S, and SO_4 were very common ions.

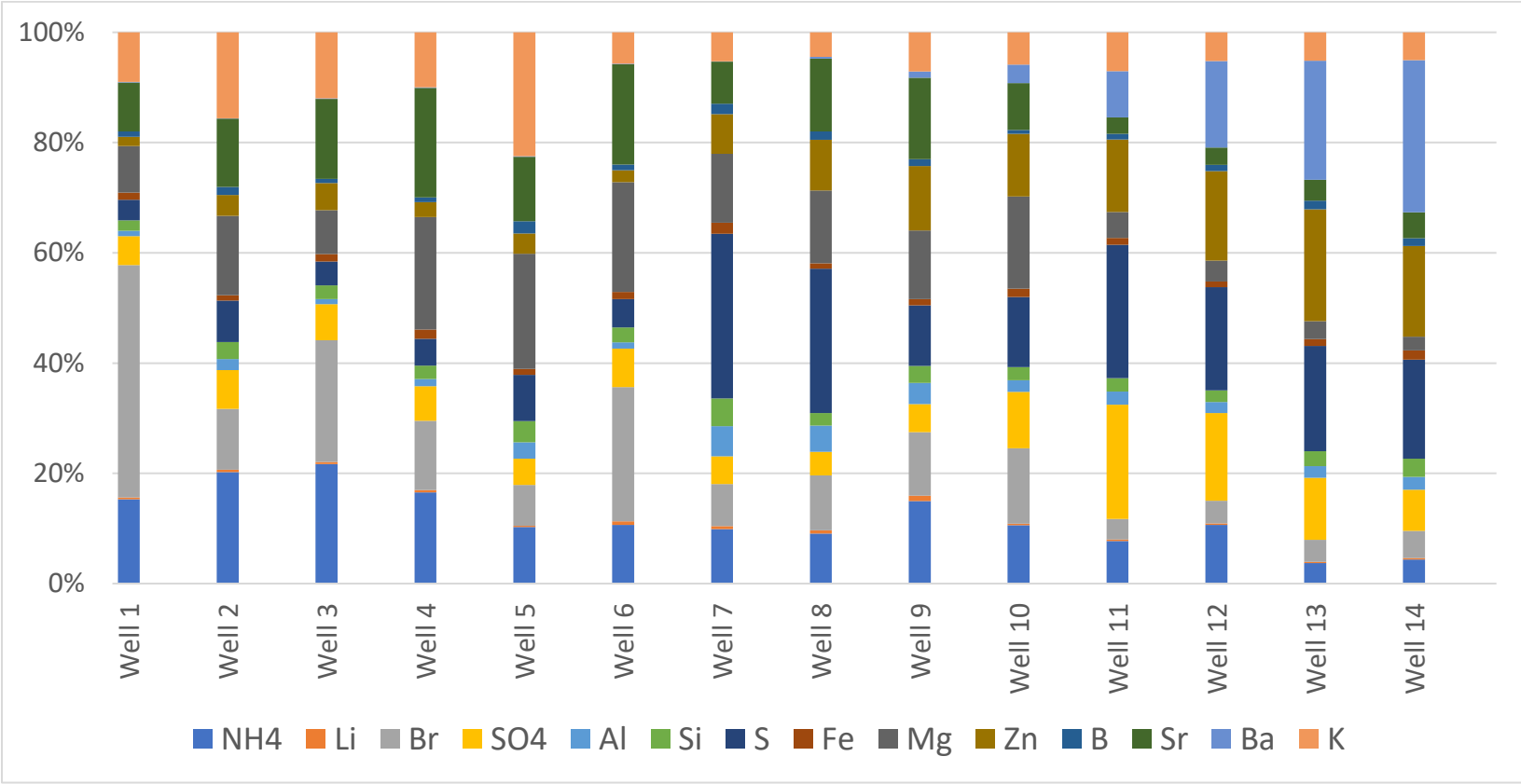

Figure 8: Distribution of ions in each sample after exclusion of Na, Ca, and Cl

Treated produced water characterization

In this study the coagulation-flocculation-sedimentation (CFS) has been selected to treat the produced water samples from three sub-basins all from Permian basin. Two coagulants were selected to be added in coagulation stage and two flocculants were tested in flocculation stage after the addition of the optimum coagulant in the coagulation step. First optimum doses of these coagulants for 14 different wells were determined. Because each water sample has different characteristics, they required different amounts of coagulants. Figure 9 shows the distribution of the optimal dose of alum and ferric sulfate. If we consider by sub-basins, then for the NM the optimal dose of alum was 360mg/L, for SM was 459 mg/L and for the Delaware was 225 mg/L. But with ferric sulfate, the optimal doses were different: for the NM was 112 mg/L, for the SM was 226 mg/L and for the Delaware was 470 mg/L. As we can see Delaware samples required the least amount of alum, but the highest amount ferric sulfate. It is interesting to note that the Well 8 sample, being the most acidic, needed the lowest amount of both coagulants.

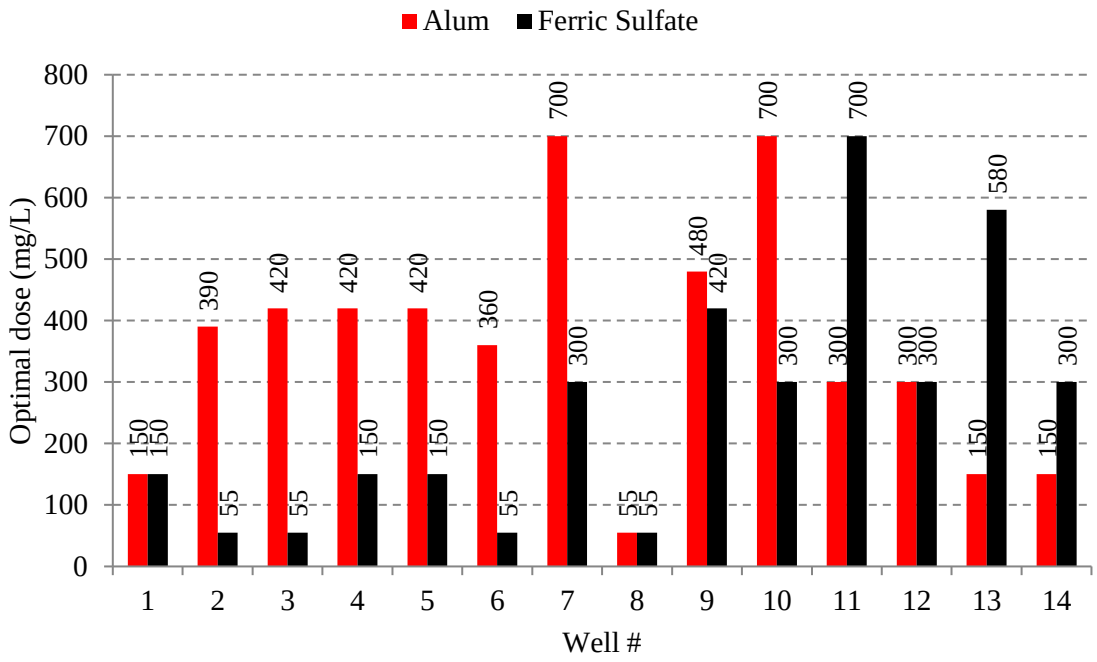

Figure 9: Summary of the optimal doses of coagulants determined through CFS process by a well

In Figures 12 and 13 we can see the effectiveness of coagulants in terms of TSS and turbidity removal. In general, the optimal dose of alum reduced TSS in the NM basin on average up to 70% and turbidity to 96%. In the SM basin, the reduction of both parameters was approximately 90%. The least reductions were determined in the Delaware basin with 70% and 83%, respectively. On the other hand, the optimal dose of ferric sulfate reduced TSS in the NM basin on average up to 87% and turbidity to 97%. In the SM basin, the reduction of TSS was 91% and turbidity 92%. Interesting to note the least reductions were determined in the Delaware basin, as in the case with alum, with 78% and 88%, respectively.

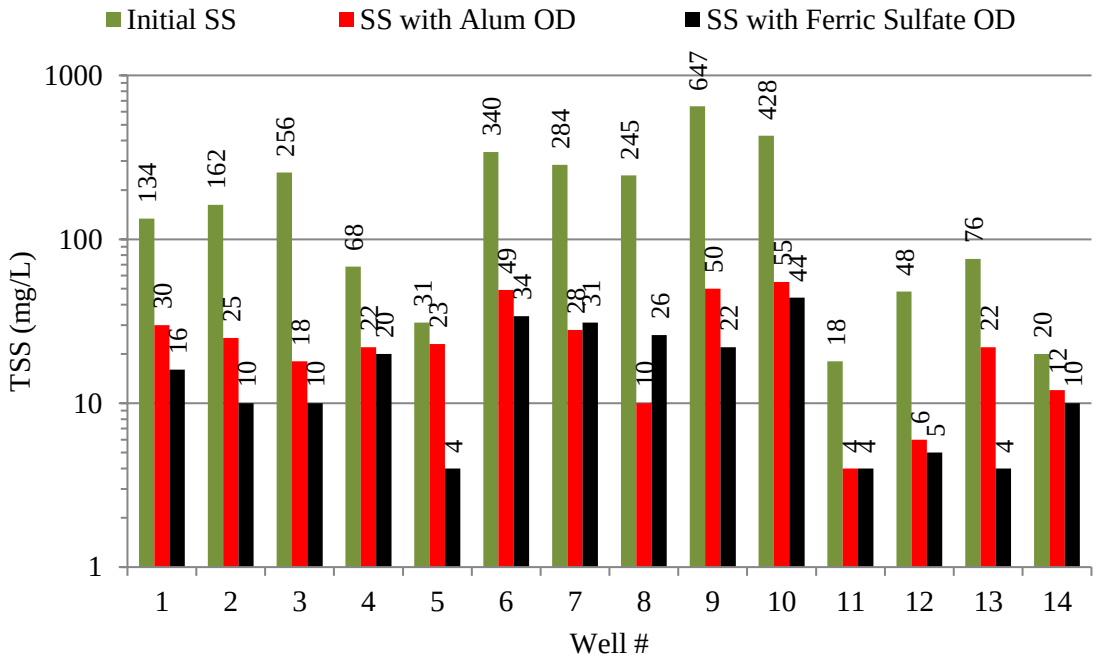

Figure 10: Comparing TSS values before and after using alum and ferric sulfate as coagulants

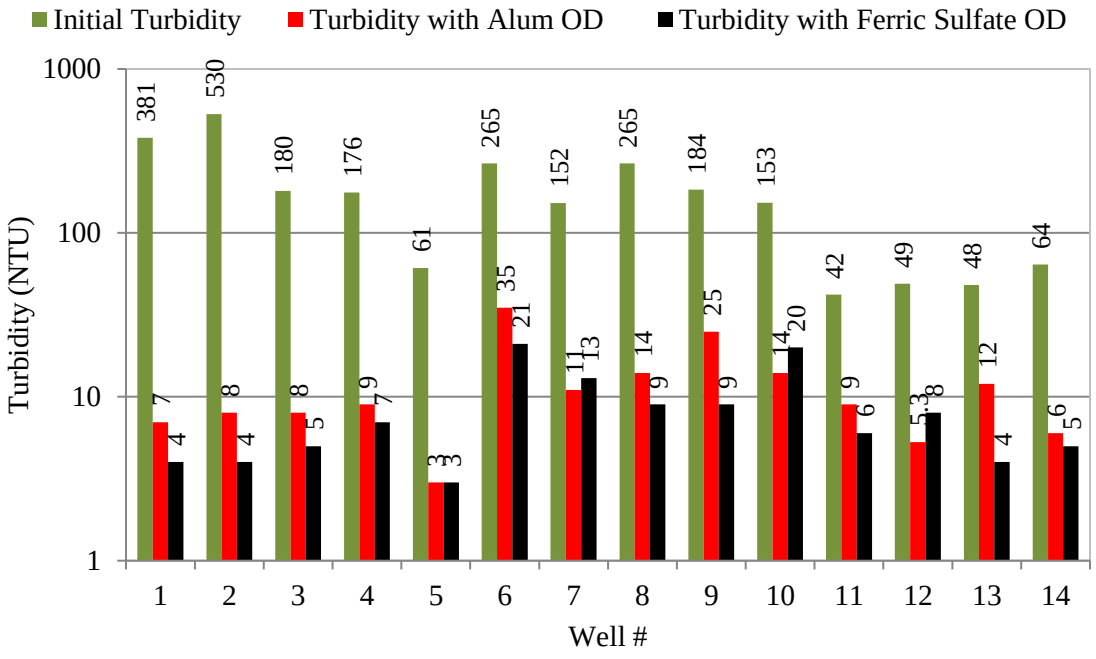

Figure 11: Comparing turbidity reduction before and after using alum and ferric sulfate as coagulants

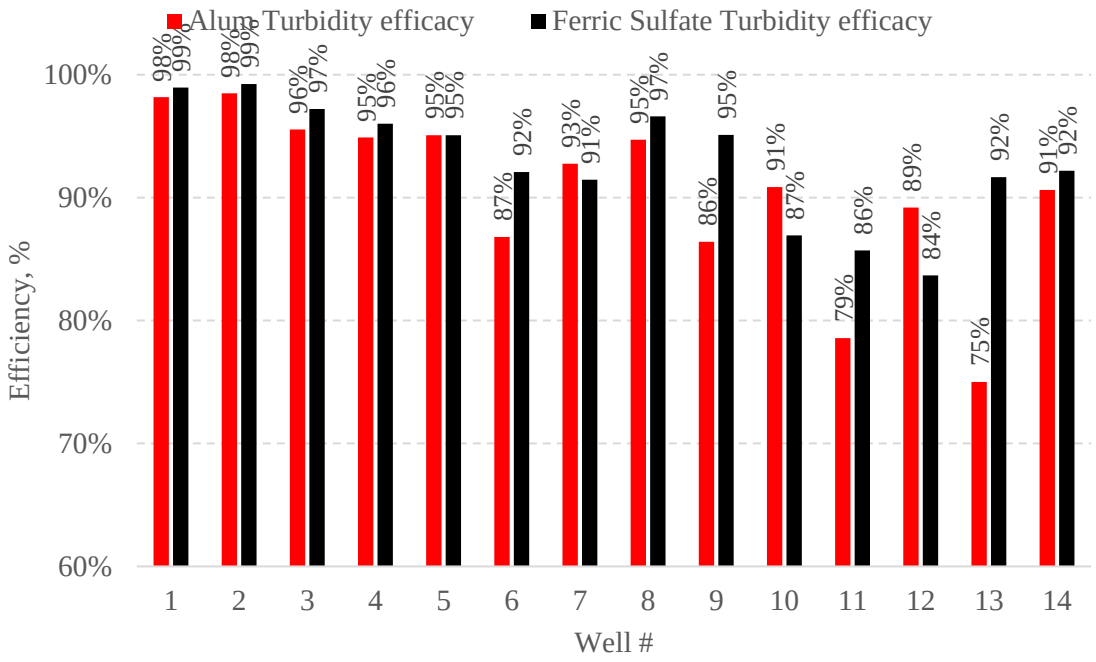

Figure 12: Efficiency of TSS reduction by using alum and ferric sulfate as coagulants

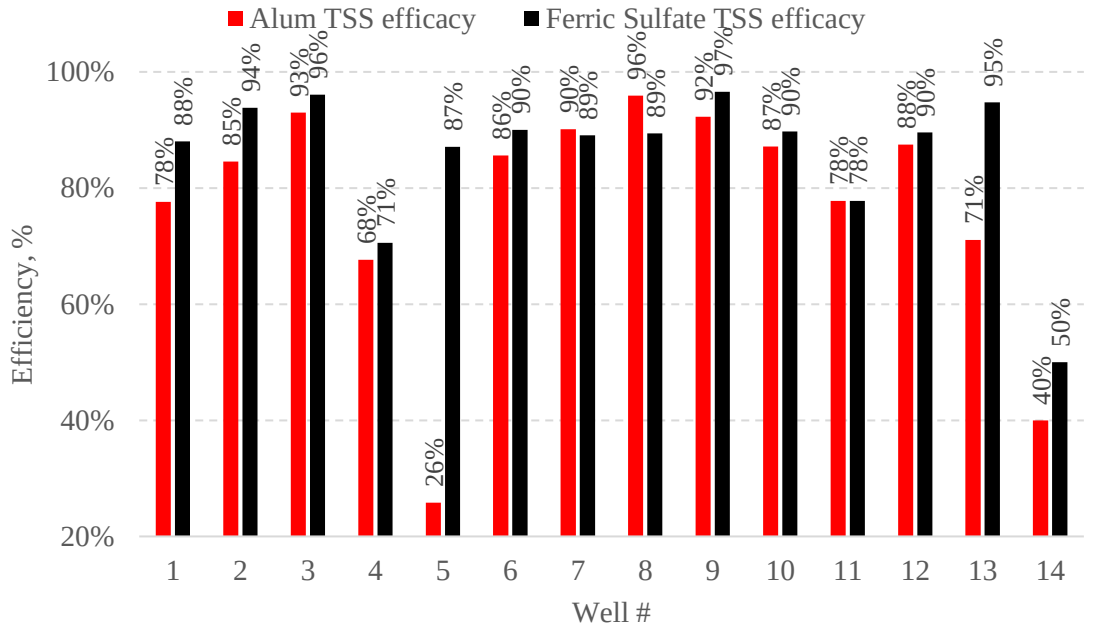

Figure 13: Efficiency of turbidity reduction by using alum and ferric sulfate as coagulants

Since there are no standards for treated water, I used a threshold TSS of 30 mg/L and turbidity of 10 NTU as described in other studies (Wilson 2016). When using alum during the CFS process, the coagulation step alone was sufficient for seven wells (Well 2, 3, 4, 5, 11, 12, 14). It was less effective compared to ferric sulfate. Ferric sulfate could reduce both TSS and turbidity to the acceptable levels of ten wells (Well 1, 2, 3, 4, 5, 8, 9, 11, 12, 13, 14).

For the other well samples, in which the coagulation step was not sufficient, two flocculants were added in the flocculation step to increase treatment efficiency. Two different flocculants were used: cationic starch and polyamine. They have been selected for their effectiveness as flocculation agents during the preparation of drilling fluids (Perkins & Craft, 1943). One single dose of 20 mg/L was tested. Cationic starch reduced TSS by an additional 3% when using alum and 2.37% when using ferric sulfate. On the other hand, polyamine reduced TSS by an additional 2.65% when using alum and 1.21% when using ferric sulfate. This means in terms of TSS reduction, both organic flocculants were not highly efficient. But it must be noted that cationic starch, compared with polyamine, not only decreased TSS slightly more but also reduced approximately 10% TDS of the samples.

More detailed experiment results in terms of total suspended solids, turbidity, and total dissolved solids removal efficiencies can be seen in Tables 9 and 10. The empty sells indicate that for those cases the coagulation step was sufficient. In the case with polyamine, there was some increase in TSS and turbidity, as marked by negative values. Cationic starch might have reduced TDS because of the high concentration of active

positive charges. Polyamine, on the other hand, did not have any effect on the TDS of samples.

Table 8: Efficiency of cationic starch as a flocculant (refer to Figure 8 for the optimal doses of coagulants)

	Cationic starch effectiveness: TSS reduction, %		Cationic starch effectiveness: Turbidity reduction, %		Cationic starch effectiveness: TDS reduction, %	
Well number	Alum	Ferric Sulfate	Alum	Ferric Sulfate	Alum	Ferric Sulfate
1	17		29		0	
6	31	29	23	29	18	14
7	11	3	18	23	13	13
8	0		21		9	
9	18		28		15	
10	20	9	29	25	5	5
13	27		17		8	

Table 9: Efficiency of polyamine as a flocculant (refer to Figure 9 for the optimal doses of coagulants)

	Polyamine effectiveness: TSS reduction, %		Polyamine effectiveness: Turbidity reduction, %		Polyamine effectiveness TDS: reduction, %	
Well number	Alum	Ferric Sulfate	Alum	Ferric Sulfate	Alum	Ferric Sulfate
1	20		-14		0	
6	29	12	0	14	3	2
7	11	3	9	0	-1	-2
8	-20		29		-2	
9	12		20		-4	
10	27	20	29	25	-3	-3
13	18		17		1	

Statistical results

Experimental results presented in the previous two subsections for initial and treated water characterization are used to generate correlations to provide quick treatment recipes for oil field waters originated during production. I used Pearson correlation to describe their relations.

In Figure 14 we can see positive Pearson correlation coefficients between parameters of initial PW and Optimal dose for coagulants. The intersection of ZP and TDS indicates that when zeta potential decreases, the amount of TDS increases. This might be because of the high concentration of elements which increases the chance of collision and adhering to each other. The scatter plot of this relation can be found in Figure 15.

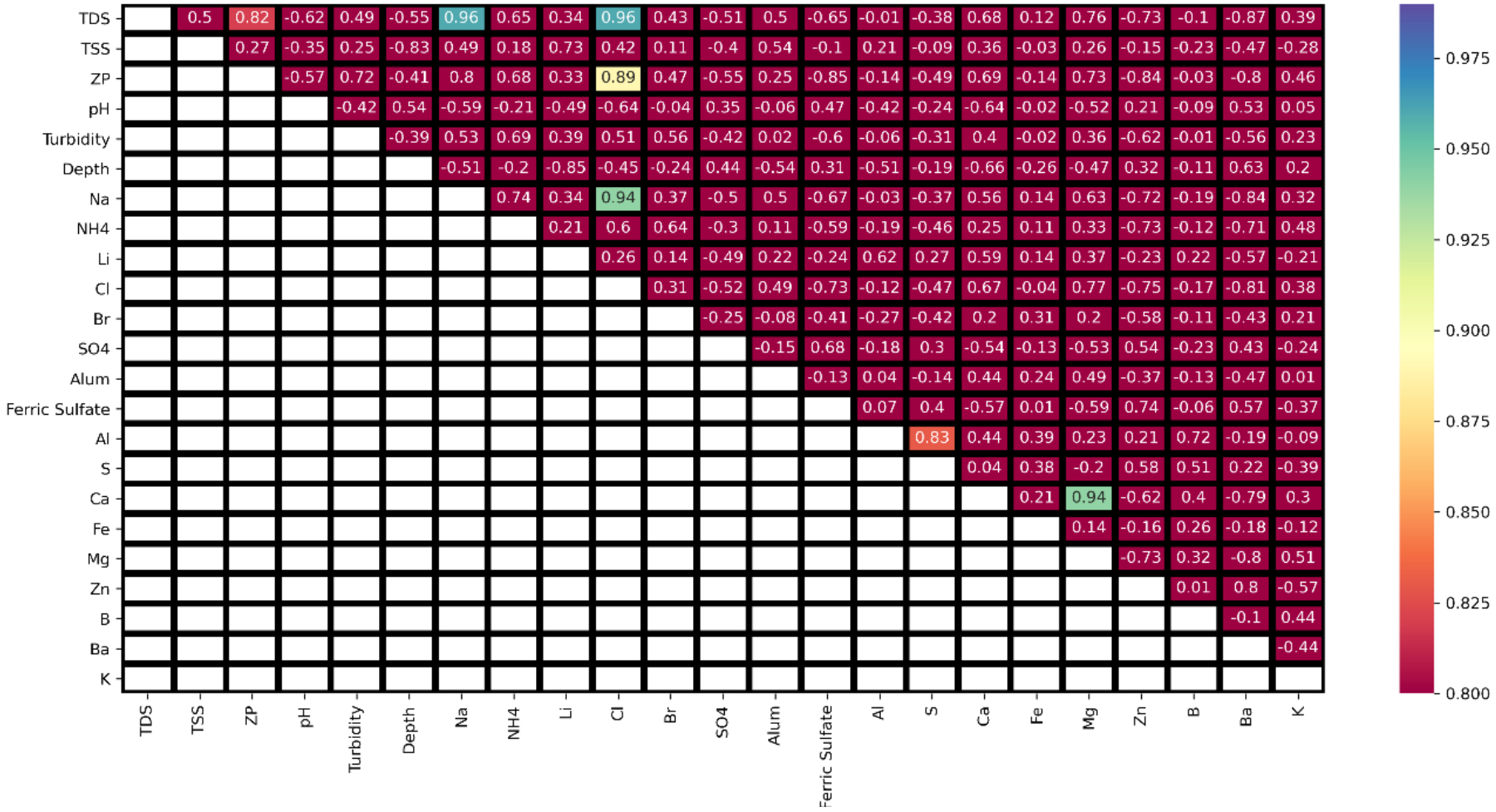

Figure 14: Positive Pearson correlation coefficients obtained from heatmap that describes the connection between PW sample parameters including Optimal dose

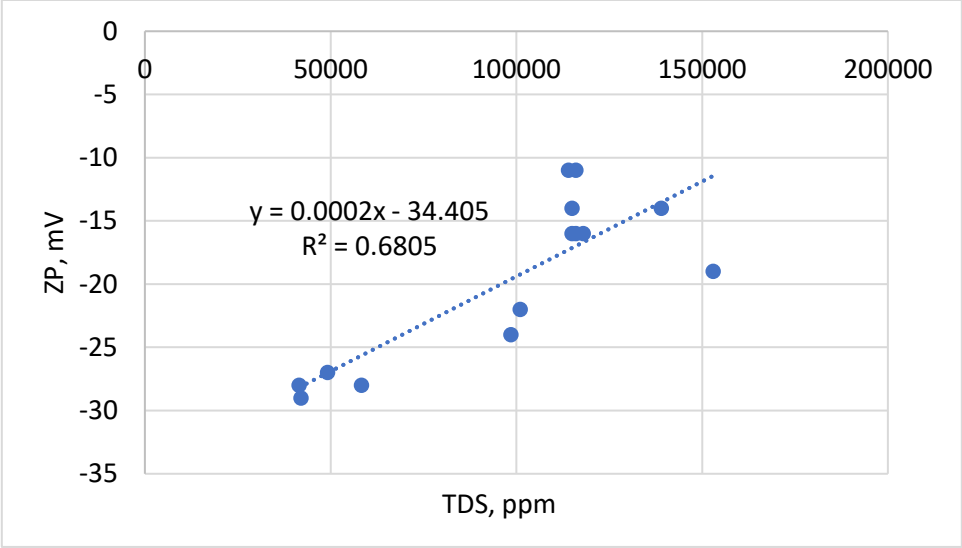

Figure 15: Correlation between Zeta potential and TDS in the produced water samples ($y = 0.0002x - 34.405$ and $R^2 = 0.6805$)

Ca^+ and Mg^+ ions also were linearly correlated. Probably this was due to interaction between PW and dolomite rocks in reservoir formation. The scatter plot of this relation can be found in Figure 16.

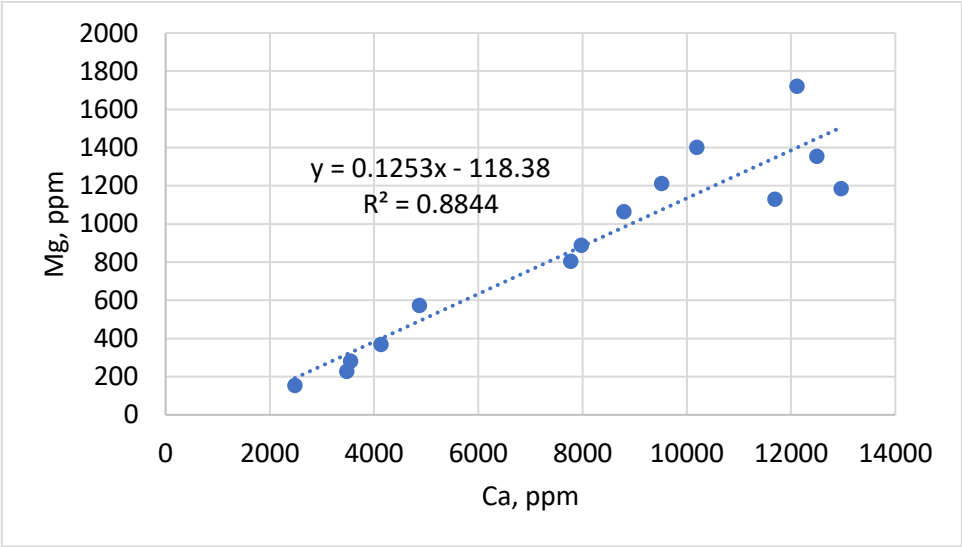

Figure 16: Relation between Mg and Ca ions in the produced water samples ($y = 0.1253x - 118.38$ and $R^2 = 0.8844$)

The clearest association was between TDS and Na^+ and Cl^- ions. This tells that TDS mainly consists of Na and Cl elements. The scatter plot of this relation can be found in Figure 17.

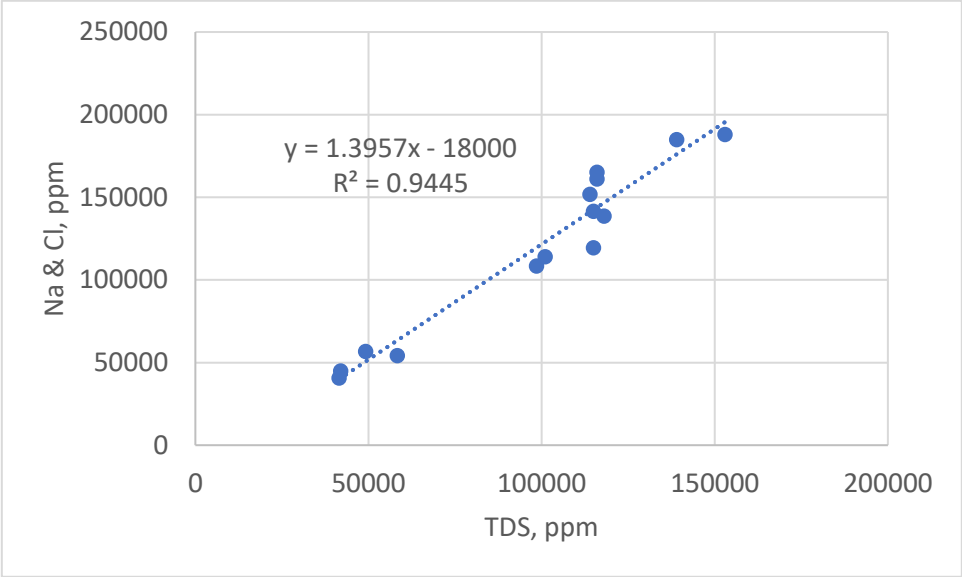

Figure 17: Relation between Na & Cl ions and TDS in the produced water samples (y = 1.3957x – 18000 and R^2 = 0.9445)

In Figure 18 we can see negative Pearson correlation coefficients. It is obvious that TSS decreased with increasing depth. This might be due to the fact that more compacted rocks under high pressure and temperature release fewer loose particles than in upper formations. The scatter plot of this relation can be found in Figure 19.

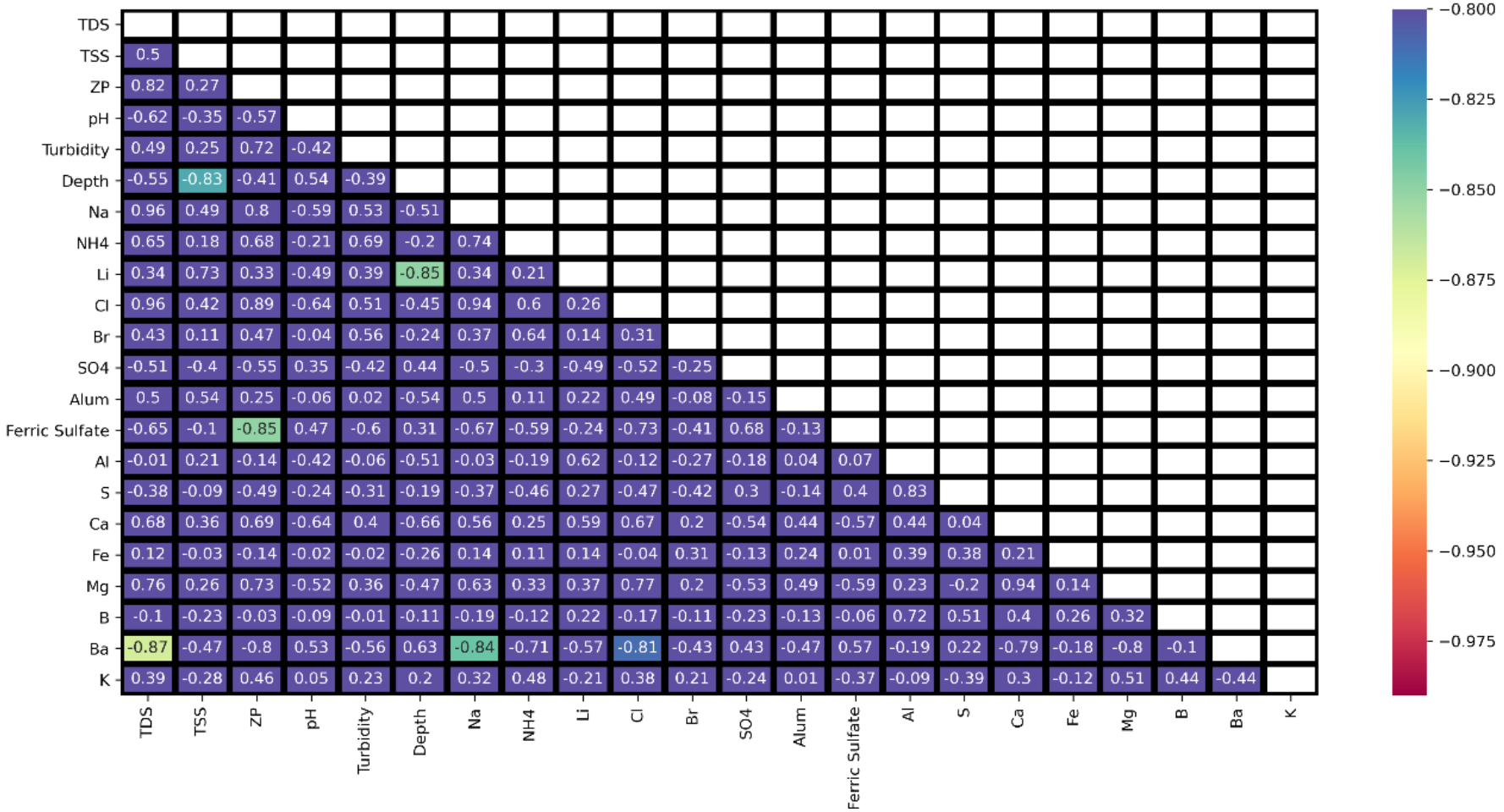

Figure 18: Negative Pearson correlation coefficients obtained from heatmap that describes the connection between PW sample parameters including Optimal dose

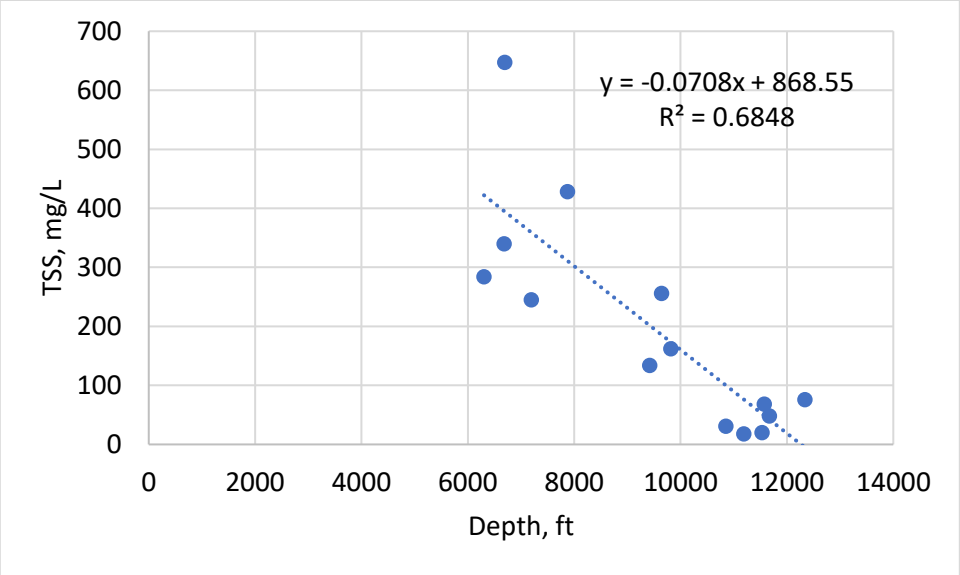

Figure 19: Relation between TSS and Depth in the produced water samples (y = -0.0708x + 868.55 and R^2 = 0.6848)

It is interesting to note highly pursued lithium (Li) was decreasing with depth. It might be due to the geologic characteristic of the formation during sedimentation. The scatter plot of this relation can be found in Figure 20.

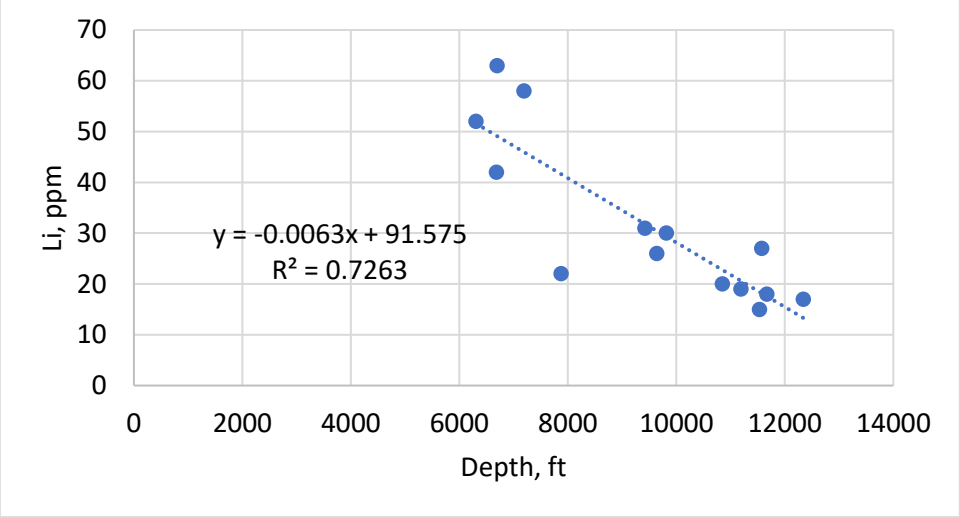

Figure 20: Relation between Li ion and Depth in the produced water samples (y = -0.0063x + 91.575 and R^2 = 0.7263)

The amount of ferric sulfate needed to coagulate the samples depended on their zeta potential. More negative ZP was, more coagulant was required. But in the case of alum, there was not any such correlation. The scatter plot of this relation can be found in Figure 21.

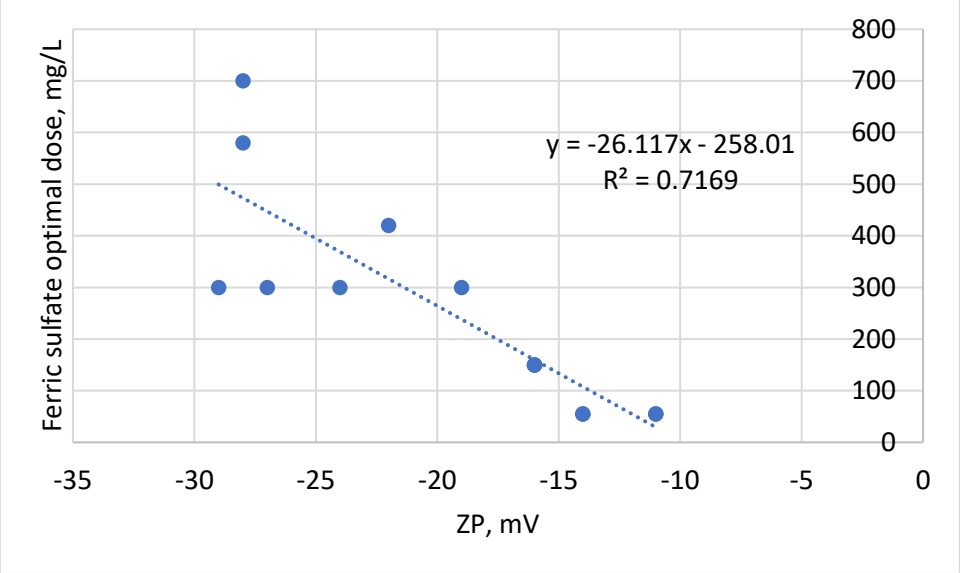

Figure 21: Relation between Ferric sulfate optimal dose and ZP in the produced water samples (y = -26.117x - 258.01 and R^2 = 0.7169)

Though there are no established direct correlations between TDS and pH, in this study high TDS corresponded to lower pH. This might be caused by an increased proportion of carbon dioxide during precipitation of this high TDS aquatic layer. The scatter plot of this relation can be found in Figure 22.

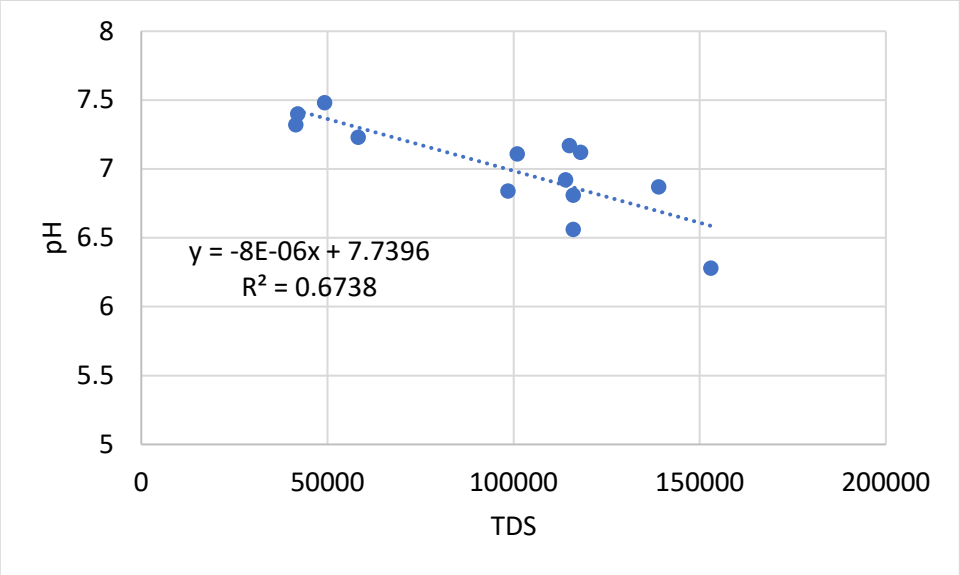

Figure 22: Relation between pH and TDS in the produced water samples (y = -8E-06x + 7.7396 and R^2 = 0.6738)

CHAPTER IV

CONCLUSIONS

As a result of the study, several conclusions were made:

1. North Midland and South Midland sub-basins, unlike the Delaware basin, required a larger amount of alum coagulants than ferric sulfate. That means it is better to use ferric sulfate in Midland sub-basins and alum in Delaware. Because fewer chemicals we add, less sludge and slighter pH decrease will occur.

2. The amount of ferric sulfate needed to coagulate the samples depended on the ZP of the initial PW. Samples with more negative ZP required more coagulant doses. But in the case of alum, there was not any such correlation.

3. More than 90% of TDS in all samples were due to NaCl minerals.

5. Permian PW samples, based on the Thermogravimetric analysis results, have an undetectable portion of dispersed organic matter. Those organics that are present are large enough to be separated by gravity force and floatation.

6. Because of the specifications of water, not all organic flocculants might be effective for Permian PW. In my study, despite their high price and good reputation, the chosen flocculants could not reduce TSS significantly. Thus, each chemical should be tested by Jar test (or other standard methods) to meet efficacy expectations.

7. Further research needed to understand Cationic starch's effect on potentially reducing the TDS amount in the Permian PW. Because of its high price, it cannot be used in a field. But if the mechanism can be determined behind the detected TDS reduction, it is possible

to find those triggers in much cheaper chemicals. TDS reduction and the role of constituents are out of the scope of this research.

8. Pearson correlation can be used to determine other relations between different parameters. If sufficient data is collected, it can be used to generate more detailed causation models.

To summarize, reinjection of produced waters for hydraulic fracturing purposes can be considered if the total suspended solids (TSS) can be removed from the waters. Because TSS can be very prompt for precipitation and may cause plugs in open features and may reduce fracture size which has been created for hydrocarbons to flow. This study concluded that TSS can effectively be removed from produced water samples by using coagulation-flocculation-sedimentation (CFS) process. It has also concluded that ferric sulfate is a very effective coagulant to remove TSS in the South and North Midland sub-basins and the Delaware basin. Flocculants used in this study could not improve CFS performance. However, the cationic starch use as a flocculant coupled with mostly ferric sulfate has proven to be an effective TDS remover.

REFERENCES

A case study: Effective fracturing with recycled water. Halliburton helped Permian Basin operator save more than $500,000 and 8,000,000 gallons of water. 2013 Halliburton. H09855

Abdou, M., Carnegie, A., Mathews G. et al. 2011. Finding value in formation water. Oilfield review. https://www.slb.com/-/media/files/oilfield-review/finding-value (accessed October 2021)

Aften, C.W. and Zhang, Y.J. 2016. Possibility of Flooding Polymer or Water Reuse via Innovative Selective or Total Flocculation of Enhanced Oil Recovery Produced Water. Paper presented at the SPE Improved Oil Recovery Conference, Tulsa, Oklahoma, USA, April 11–13. SPE-179525-MS. https://doi.org/10.2118/179525-MS

Akash, M., Rehman, K., Chen, S. 2014. Natural and Synthetic Polymers as Drug Carriers for Delivery of Therapeutic Proteins. Polymer Reviews, pp 371-406. https://doi.org/10.1080/15583724.2014.995806

Ali, M. and Hascakir, B. 2018. Water/Rock Interaction for Eagle Ford, Marcellus, Green River, and Barnett Shale Samples and Implications for Hydraulic-Fracturing-Fluid Engineering. SPE J. 22: 162–171. https://doi.org/10.2118/177304-PA

Ali, M., Banerjee, S., Hascakir, B. 2016. The Environmental Aspect of Produced Water Management for the Oil Field Waters Originated Thermal EOR, SPE International Heavy Oil Conference & Exhibition, 6-8 December, Mangaf, Kuwait, SPE-184139-MS.

Ali, M., Hascakir, B., A Critical Review of Emerging Challenges for the Oil Field Waters in United States, SPE E&P Health, Safety, Security, and Environmental Conference-Americas, 16-18 March 2015, Denver, Colorado, USA, SPE 173529-MS.

Altaher, H., ElQada, E., Omar W. 2011. Pretreatment of Wastewater Streams from Petroleum/Petrochemical Industries Using Coagulation. Advances in Chemical Engineering and Science 1(4): 245–251. https://doi:10.4236/aces.2011.14035

Bureau of Economic geology, University of Texas. https://www.beg.utexas.edu/research/programs/starr/unconventional-resources/wolfberry-spraberry (accessed October 2021)

Bolto, B. and Gregoryba, J. 2007. Organic polyelectrolytes in water treatment. Water Research 41(11): 2301-2324. https://doi.org/10.1016/j.watres.2007.03.012

Brandt M.J., Johnson, K.M., Elphinston, A.J. 2016. Twort's Water Supply, seventh edition. Butterworth–Heinemann/Elsevier. https://doi.org/10.1016/C2012-0-06331-4

Brown T.C., Mahat V., Ramirez J.A. 2019. Adaptation to future water shortages in the United States caused by population growth and climate change. Earth's future, 7, 219-234. https://doi.org/10.1029/2018EF001091

Buck, J.D. 1974. Effects of medium composition on the recovery of bacteria from sea water. Journal of Experimental Marine Biology and Ecology, Volume 15, Issue 1, Pages 25-34. https://doi.org/10.1016/0022-0981(74)90060-4.

Chapin, F.S., Matson, P.A., Vitousek, P.M. 2011. Principles of Terrestrial Ecosystem Ecology. 2nd Edn. New York, NY: Springer.

Chaudhary, B.K., Willman, S.E., Carroll, K.C. 2016. Spatial Variability and Geochemistry of Produced Water in Southeastern New Mexico, USA. https://nmwrri.nmsu.edu/wp-content/uploads/ProducedWater-Reports/Reports/ (accessed April 2021)

Correlation (Pearson, Kendall, Spearman). https://www.statisticssolutions.com/free-resources/directory-of-statistical-analyses/correlation-pearson-kendall-spearman (accessed September 2021)

Dahm, K.and Chapman, M. 2014. Produced Water Treatment Primer: Case Studies of Treatment Applications. Bureau of Reclamation.

Enverus. US Oil production 2020. https://app.drillinginfo.com/production/#/default (accessed August 2021)

Environmental and Energy Study Institute. Fossil Fuels. https://www.eesi.org/topics/fossil-fuels/description (accessed July 2021)

Esmaeilirad, N., Terry, C., Kennedy, H. et al. 2016. Recycling Fracturing Flowback Water for Use in Hydraulic Fracturing: Influence of Organic Matter on Stability of Carboxyl-Methyl-Cellulose-Based Fracturing Fluids. SPE J. 21: 1358–1369. https://doi.org/10.2118/179723-PA

Fang, C.S., and Lin, J.H. 1988. Air Stripping for Treatment of Produced Water. J Pet Technol 40: 619–624. https://doi.org/10.2118/16328-PA

Farajnezhad, H. and Gharbani, P. 2012. Coagulation treatment of wastewater in petroleum industry using poly aluminum chloride and ferric chloride. Arpapress. IJRRAS 13(1)

Gregory, K.B., Vidic, R.D., Dzombak, D.A. 2011. Water Management Challenges Associated with the Production of Shale Gas by Hydraulic Fracturing. Elements 7(3): 181–186. https://doi.org/10.2113/gselements.7.3.181.

Guerra, K., Dahm, K., Dundorf, S. 2011. Oil and Gas Produced Water Management and Beneficial Use in the Western United States. Science and Technology Program Report No. 157. Prepared for Reclamation Under Agreement No. A10-1541-8053-381-01-0-1, Denver, Colorado.

Hardy, W.B. 1900. A Preliminary Investigation of the Conditions Which Determine the Stability of Irreversible Hydrosols. J.Phys. Chem. 4(4): 235–253. https://doi.org/10.1021/j150022a001.

Hascakir, B. 2003. Utilization of Natural Polyelectrolytes in wasterwater treatement. MSc Thesis. Izmir, Turkey

Hascakir, B., Dolgen, D., Utilization of Clay Minerals in Wastewater Treatment: Organic Matter Removal with Kaolinite, Ekoloji, 66 (6), 47-54, 2008 (Turkish). Q3, IF: 0.708, SJR: 11677, H: 11.

Hassan, A.A. and Mousa, K.M. 2017. Oilfield Produced Water Treatment by Coagulation /Flocculation Processes. The Second Conference of Post Graduate Researches. College of Engineering, Al-Nahrain University, Baghdad, Iraq

Hassinger, E., Doerge, T.A., Baker, P.B. 1994. Water Facts: Number 6 Reverse osmosis units. Publication number 194019. http://ag.arizona.edu/pubs/water/ az9419.pdf

Igunnu, E.T. and Chen, G.Z. 2012. Produced Water Treatment Technologies. International Journal of Low-Carbon Technologies 2014(9): 157–177. https://doi:10.1093/ijlct/cts049

Jiang, J., Oberdörster, G., Biswas, P. 2009. Characterization of size, surface charge, and agglomeration state of nanoparticle dispersions for toxicological studies. J Nanopart Res 11, 77–89. https://doi.org/10.1007/s11051-008-9446-4

Joseph, E. and Singhvi, G. 2019. Multifunctional nanocrystals for cancer therapy: a potential nanocarrier. Nanomaterials for Drug Delivery and Therapy. ISBN 9780128165058. https://doi.org/10.1016/B978-0-12-816505-8.00007-2.

Kaishentayev, D., Hascakir B., Reuse of Produced Waters Containing High Total Dissolved Solids (TDS) for Fracturing, SPE Annual Technical Conference and Exhibition (ATCE 2020), 21-23 September 2021, Dubai, UAE, SPE-206371-MS.

Kakadjian, S., Thompson, J., Torres, R. et al. 2013. Stable Fracturing Fluids from Waste Water. Paper presented at the SPE Unconventional Resources Conference Canada, Calgary, Alberta, Canada. https://doi.org/10.2118/167175-MS

KentState University. Pearson Correlation. https://libguides.library.kent.edu/SPSS/PearsonCorr (accessed September 2021)

Khalilpour, R. 2014. Produced Water Management: An Example of a Regulatory Gap. Paper presented at the SPE Oilfield Water Management Conference and Exhibition, Kuwait City, Kuwait. https://doi.org/10.2118/171000-MS

Kondash, A.J., Albright, E., Vengosh A. 2017. Quantity of Flowback and Produced Waters from Unconventional Oil and Gas Exploration. Science of the Total Environment 574: 314–321. https://doi.org/10.1016/j.scitotenv.2016.09.069.

Krauss, C. 2019. The "Monster" Texas Oil Field That Made the U.S. a Star in the World Market. The New York times. https://www.nytimes.com/ 2019/02/03/ business/energy-environment/texas-permian-field-oil.html (accessed July 2021)

Lancon, O. and Hascakir, B. 2018. Contribution of Oil and Gas Production in The US to The Climate Change. Paper presented at the SPE Annual Technical Conference and Exhibition, Dallas, Texas, USA, September. https://doi.org/10.2118/191482-MS

Liden T., Hildenbrand L.Z., Schug A.K. 2019. Pretreatment Techniques for Produced Water with Subsequent Forward Osmosis Remediation. Water 11(7): 1437. https://doi.org/10.3390/w11071437

Macczak, P., Kaczmarek, H. and Ziegler-Borowska, M. 2020. Recent Achievements in Polymer Bio-Based Flocculants for Water Treatment. Materials, 13(18): 3951. https://doi.org/10.3390/ma13183951

Maguire-Boyle, S.J. and Barron, A.R. 2014. Organic compounds in produced waters from shale gas wells. Environmental Science: Processes & Impacts. https://doi.org/10.1039/C4EM00376D

Malik, H.Q. 2018. Performance of Alum and Assorted Coagulants in Turbidity Removal of Muddy Water. Applied Water Science 8(40). https://doi.org/10.1007/s13201-018-0662-5

Mayerhofer, M.J., Richardson, M.F., Walker R.N et al. 1997. Proppants? We Don't Need No Proppants. Paper SPE 38611 presented at the SPE Annual Technical Conference and Exhibition, San Antonio, Texas, USA, 5-8 October. https://doi.org/10.2118/38611-MS

Montgomery, S. 1998. Thirtyone Formation, Permian Basin, Texas: Structural and Lithologic Heterogeneity in a Lower Devonian Chert Reservoir. 82(01): 1-24pp

Nasr-El-Din, H.A. 2003. New Mechanisms of Formation Damage: Lab Studies and Case Histories. Paper presented at the SPE European Formation Damage Conference, The Hague, Netherlands, May. https://doi.org/10.2118/82253-MS

NationalGeographic. https://www.nationalgeographic.com/environment/article/ fracking-water-its-just-so-hard-to-clean (accessed August 2021)

Ng, J.H., Tariq, A., Nasr-El-Din, H.A. 2018. Replacing the Use of Freshwater With Seawater: Problems, Solutions, and Applications. Paper presented at the SPE/AAPG/SEG Unconventional Resources Technology Conference, Houston, Texas, USA, July. https://doi.org/10.15530/URTEC-2018-2896321

Ojagh, S.M., Fallah, N., Nasernejad, B. 2020. Biological treatment of organic compounds in produced water with use of halotolerant bacteria. Journal of Environmental Chemical Engineering 8(6). https://doi.org/10.1016/j.jece.2020.104412

Pal, P. 2017. Industrial Water Treatment Process Technology. ISBN.978-0-12-810391-3.

Palisch, T.T., Vincent, M.C., Handren P.J. 2010. Slickwater Fracturing: Food for Thought. SPE Prod & Oper 25: 327–344. https://doi.org/10.2118/115766-PA

Pei, Y., Wang, J., Yu, W. et al. 2020. Investigation of Lateral Fracture Complexity to Mitigate Frac Hits During Interwell Fracturing. Paper presented at the SPE/AAPG/SEG Unconventional Resources Technology Conference, Virtual, July. https://doi.org/10.15530/urtec-2020-3106

Perkins, F. and Craft, B.C. 1943. Effects of Certain Gums and Starches on Filtration of Salt-water Muds at Elevated Temperatures. Trans. 151: 248–252. https://doi.org/10.2118/943248-G

Platt, F.M., Burnett, D.B., Eboagwu, U.M. et al. 2011. Pre-treatment options for frac flow back brines: laboratory and pilot plant testing of oil removal materials. Paper presented at the Canadian Unconventional Resources Conference, Calgary, Alberta, Canada. SPE-147417-MS. https://doi.org/10.2118/147417-MS

Ratnayaka, D.D., Brandt M.J., Johnson, K.M. 2009. Water Supply, sixth edition. Butterworth–Heinemann/Elsevier. https://doi.org/10.1016/B978-0-7506-6843-9.X0001-7

Reese, A. 2020. High Country news. There's a new boom in the Permian Basin—wastewater. https://www.hcn.org/articles/water-theres-a-new-boom-in-the-permian-basin-wastewater

Ren21: Global Overview. Figure 1–Estimated renewable share of total final energy consumption. https://www.ren21.net/gsr-2019/chapters/chapter_01/ chapter_01 (accessed June 2021)

Renpu, W. 2011. Advanced Well Completion Engineering, 3rd edition. ISBN 978-0-12-385868-9. https://doi.org/10.1016/C2010-0-66820-9

Reynolds, R.R. 2003. Produced Water and Associated Issues: a manual for the independent operator. Oklahoma Geological Survey Open-File Report 6-2003

Rodriguez, A.Z., Wang, H., Hu, L. et al. 2020. Treatment of Produced Water in the Permian Basin for Hydraulic Fracturing: Comparison of Different Coagulation Processes and Innovative Filter Media. Water 12(770). https://doi.org/10.3390/w12030770

Sahu, O.P. and Chaudhari, P.K. 2013. Review on Chemical treatment of Industrial Waste Water. August 2013. Journal of Applied Sciences and Environmental Management 17(2). https://doi.org/10.4314/jasem.v17i2.8

Saller, A. and Stueber, A. 2018. Evolution of formation waters in the Permian Basin, United States: Late Permian evaporated seawater to Neogene meteoric water. AAPG Bulletin. 102. 401-428. 10.1306/0504171612517157.

Scanlon, B.R., Ikonnikova, S., Yang, Q. 2020. Will Water Issues Constrain Oil and Gas Production in the United States? Environ. Sci. Technol. 54(6): 3510–3519. https://doi.org/10.1021/acs.est.9b06390

Scanlon, B.R., Reedy, R.C., Male, F. et al. 2017. Water Issues Related to Transitioning from Conventional to Unconventional Oil Production in the Permian Basin. Environ. Sci. Technol. 51(18): 10903–10912. https://doi.org/10.1021/acs.est.7b02185

Scanlon, B.R., Weingarten, M.B., Murray, K.E. et al. 2018. Managing Basin-Scale Fluid Budgets to Reduce Injection-Induced Seismicity from the Recent U.S. Shale Oil Revolution. Seismological Research Letters; 90 (1): 171–182. https://doi.org/10.1785/0220180223

Shiklomanov, I.A. 2009. Appraisal and Assessment of World Water Resources. https://doi.org/10.1080/02508060008686794

Smith, C.H. and Ziane, L. 2012. Effective Fracture Treatment Determination in Unconventional Reservoirs. Paper presented at the SPE Asia Pacific Oil and Gas Conference and Exhibition, Perth, Australia. https://doi.org/10.2118/158349-MS

Statisticssolutions.com. https://www.statisticssolutions.com/free-resources/directory-of-statistical-analyses/pearsons-correlation-coefficient (accessed September 2021)

Subhash C.A. and Yousef A.A. 2016. A Critical Review of Alternative Desalination Technologies for Smart Waterflooding. Oil & Gas Fac 5: No Pagination Specified. https://doi.org/10.2118/179564-PA

Tariq, A., AlKhaldi, M., Ng, J.H. et al. 2019. Design and Application of High-Temperature Raw-Seawater-Based Fracturing Fluids. SPE J. 24: 1929–1946. https://doi.org/10.2118/195597-PA

Tatsi, A.A., Zouboulis, A.I., Matis, K.A. et al. 2003. Coagulation/Flocculation Pretreatment of Sanitary Landfill Leachates. Chemosphere 53(7): 737–744. https://doi.org/10.1016/S0045-6535(03)00513-7

Texas RRC: Permian Basin. https://www.rrc.texas.gov/oil-and-gas/major-oil-and-gas-formations/permian-basin (accessed September 2021)

The Aluminum Association. https://www.aluminum.org/aluminum-advantage/facts-glance (accessed September 2021)

The element Iron. JLab. https://education.jlab.org/itselemental/ele026.html (accessed September 2021)

Turbidity and water. https://www.usgs.gov/special-topic/water-science-school/science/turbidity-and-water?qt-science_center_objects=0#qt-science_center_objects (accessed July 2021)

US EIA. 2019. EIA projects nearly 50% increase in world energy usage by 2050, led by growth in Asia. https://www.eia.gov/todayinenergy/detail.php?id=41433 (accessed June 2021)

US EIA. 2019. The US leads global petroleum and natural gas production with record growth in 2018. https://www.eia.gov/todayinenergy/ detail.php?id=40973 (accessed June 2021)

US EIA. 2019. U.S. crude oil production surpassed 12 million barrels per day in April. https://www.eia.gov/todayinenergy/detail.php?id=40032 (accessed October 2021)

US EIA. 2020. Texas's Midland Basin accounted for 15% of U.S. crude oil production in 2020. https://www.eia.gov/todayinenergy/detail.php?id=49076 (accessed September 2021)

US EIA. 2021. Texas State Energy Profile. https://www.eia.gov/state/ print.php?sid=TX (accessed June 2021)

Van Oort, E., van Velzen, J., Leerlooijer K. 1993. Impairment by Suspended Solids Invasion: Testing and Prediction. SPE Prod & Fac 8: 178–184. https://doi.org/10.2118/23822-PA

Veil, J. 2020. U.S. Produced Water Volumes and Management Practices in 2017. Prepared for the Ground Water Research and Education Foundation.

Veil, J., Puder, M., Elcock, D. et al. 2004. A white paper describing produced water from production of crude oil, natural gas, and coal bed methane. U.S. Department of energy, National Energy Technology Laboratory. Prepared by Argonne National Laboratory. 10.2172/821666.

Veil, J.A. and Clark E.E. 2011. Produced Water volume Estimates and Management Practices. SPE Prod & Oper 26: 234–239. doi: https://doi.org/10.2118/125999-PA

Vidic, R.D., Brantley, S.L., Vandenbossche, J.M. et al. 2013. Impact of Shale Gas Development on Regional Water Quality. Science 340(6134): 1235009. https://doi.org/10.1126/science.1235009

Waite, M. 2010. Sustainable Water Resources in the Built Environment. ISBN13:9781843393238.

Walton, N.R. 1989. Electrical Conductivity and Total Dissolved Solids—What is Their Precise Relationship? Desalination 72 (3): 275-292, ISSN 0011-9164, https://doi.org/10.1016/0011-9164(89)80012-8.

Wilson, A. 2016. Fit-for-Purpose Treatment of Produced Water for Hydraulic Fracturing in the Permian Basin. J Pet Technol 68: 67–69. https://doi.org/10.2118/1216-0067-JPT

Ye, X., Tonmukayakul, N., Lord, P. 2013. Effects of Total Suspended Solids on Permeability of Proppant Pack. Paper presented at the SPE European Formation Damage Conference & Exhibition, Noordwijk, The Netherlands. https://doi.org/10.2118/165085-MS

Yong, C., Wu, O., Xiao, J.H. et al. 2012. Re-injecting Produced Water into Tight Oil Reservoirs. Paper presented at the SPE Canadian Unconventional Resources Conference, Calgary, Alberta, Canada. SPE-162863-MS. https://doi.org/ 10.2118/162863-MS

Zhang, L. and Hascakir, B. 2020. A Systematic Study of Water-Rock Reactions to Reveal the Relationship Between Total Dissolved Solids and Colloidal System Parameters. Paper presented at the SPE Canada Unconventional Resources Conference, Virtual. doi: https://doi.org/10.2118/200013-MS

Zhang, L., Hascakir, B., A Review of Issues, Characteristics, and Management for Wastewater due to Hydraulic Fracturing in the U.S., Journal of Petroleum Science and Engineering.

Zhang, L., Tice, M., Hascakir, B. 2020. A Laboratory Study of the Impact of Re-Injecting Flowback Fluids on Formation Damage in the Marcellus Shale, SPE Journal, Volume 25-02, SPE-195336-PA.

Zhang, L., Tice, M., Hascakir, B., The Impact of Re-injection of Flowback Fluid on Formation Damage of Marcellus Shale, SPE Western Regional Meeting, 23-26 April 2019, San Jose, California, USA, SPE-195336-MS.

APPENDIX A

XRD RESULTS OF RESIDUES OF PRODUCED WATER SAMPLES

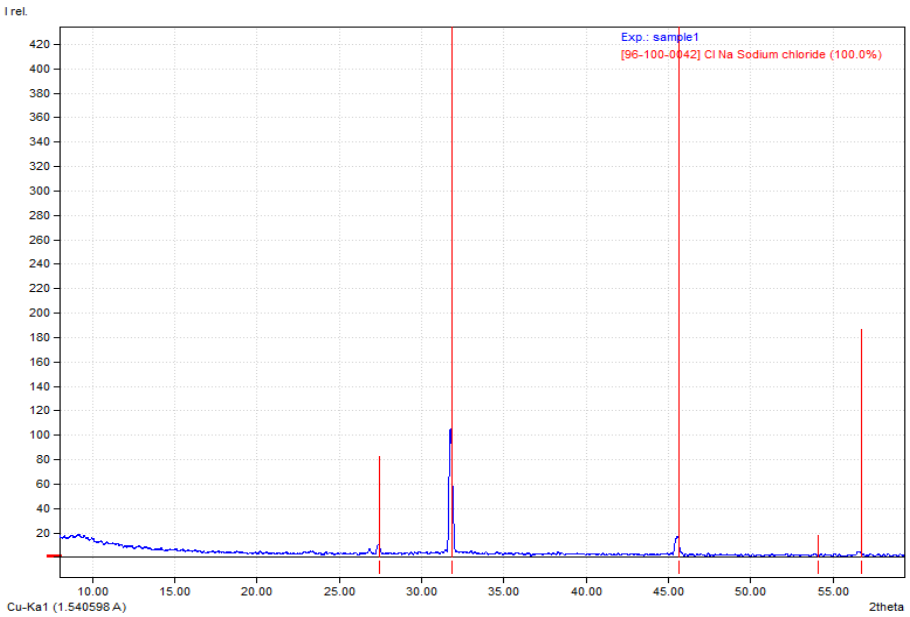

Figure 23: XRD analyses of Well 1

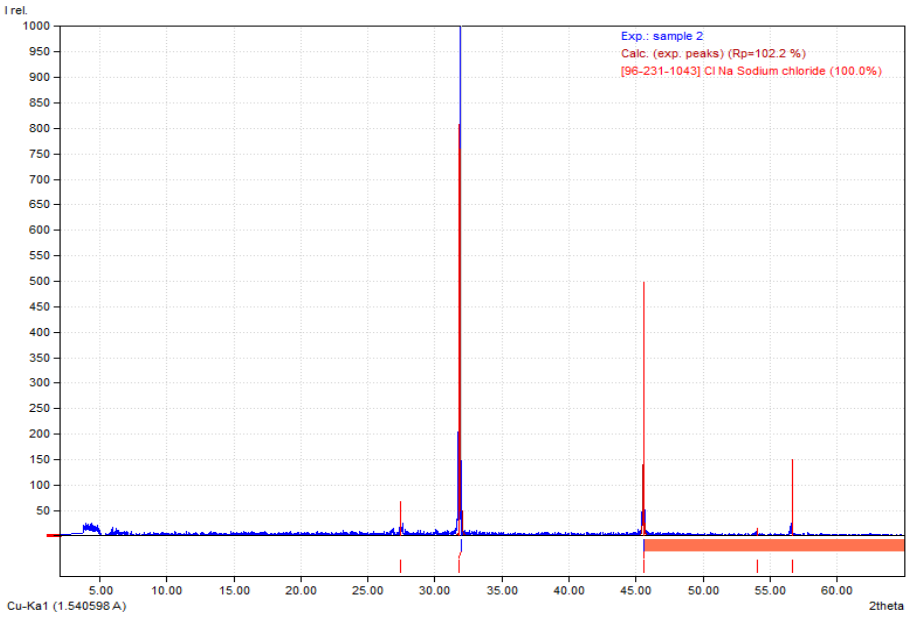

Figure 24: XRD analyses of Well 2

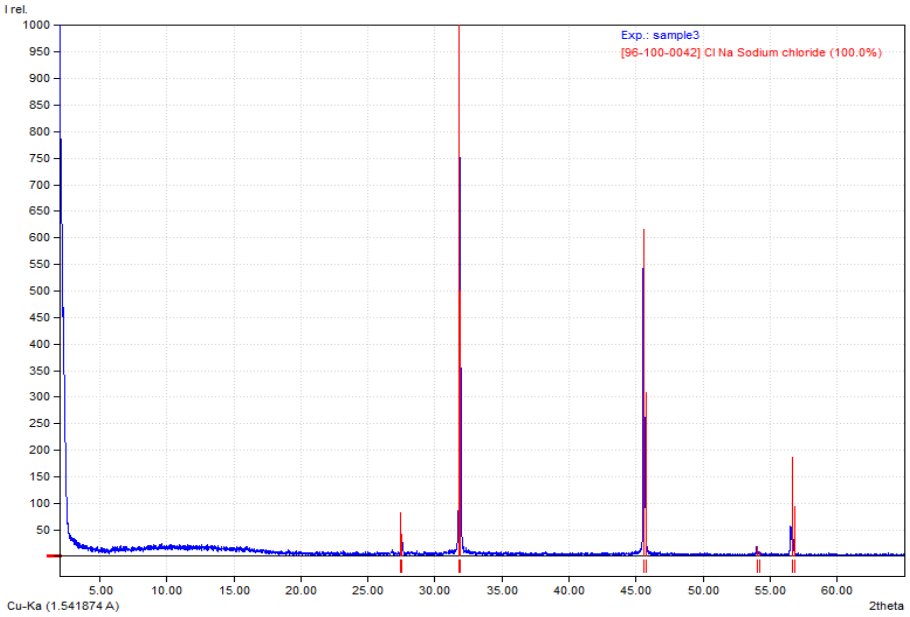

Figure 25: XRD analyses of Well 3

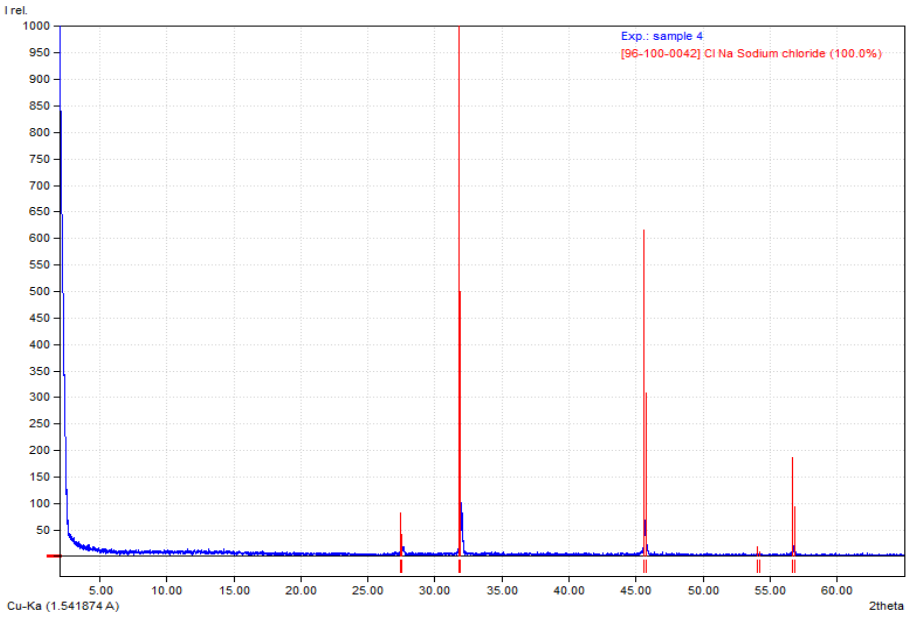

Figure 26: XRD analyses of Well 4

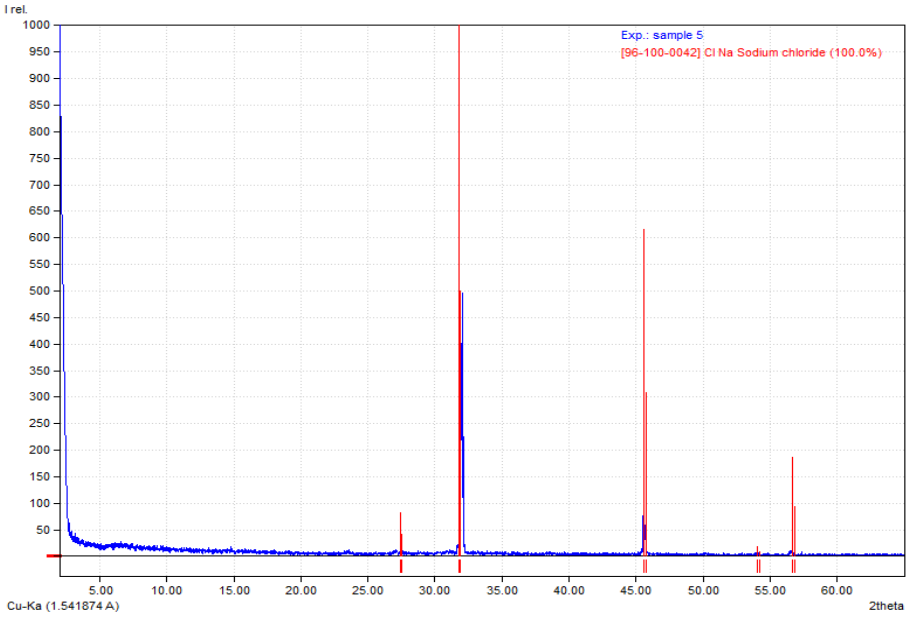

Figure 27: XRD analyses of Well 5

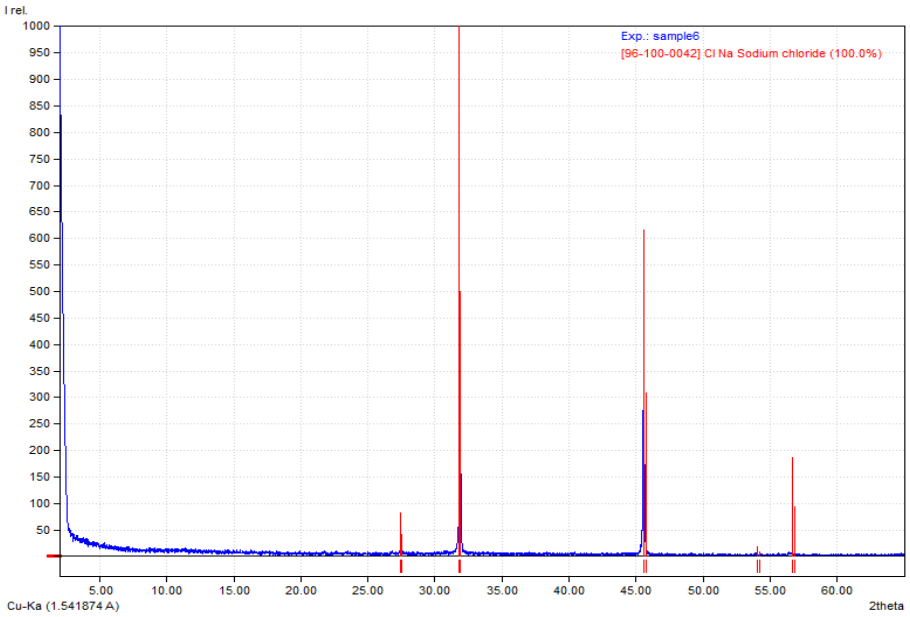

Figure 28: XRD analyses of Well 6

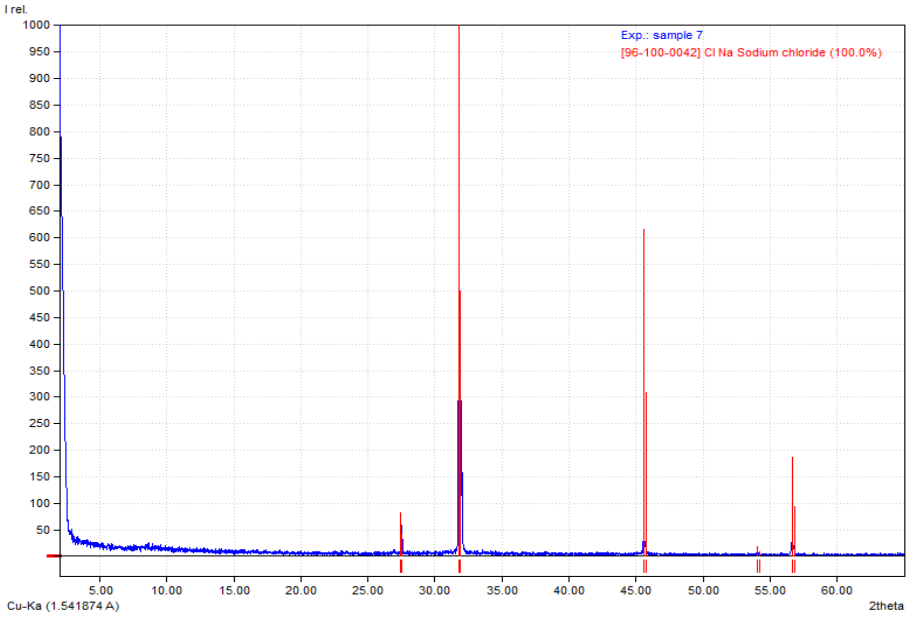

Figure 29: XRD analyses of Well 7

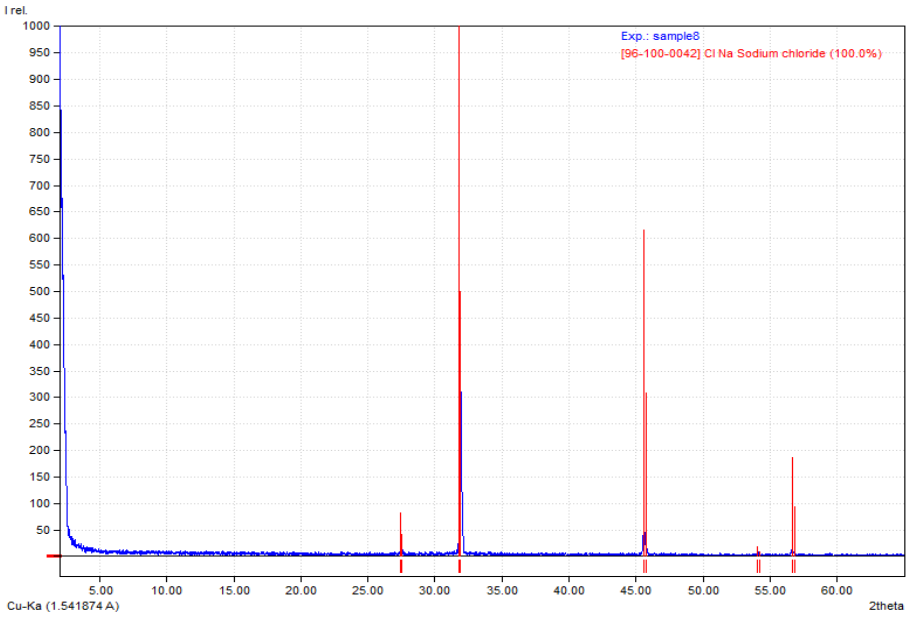

Figure 30: XRD analyses of Well 8

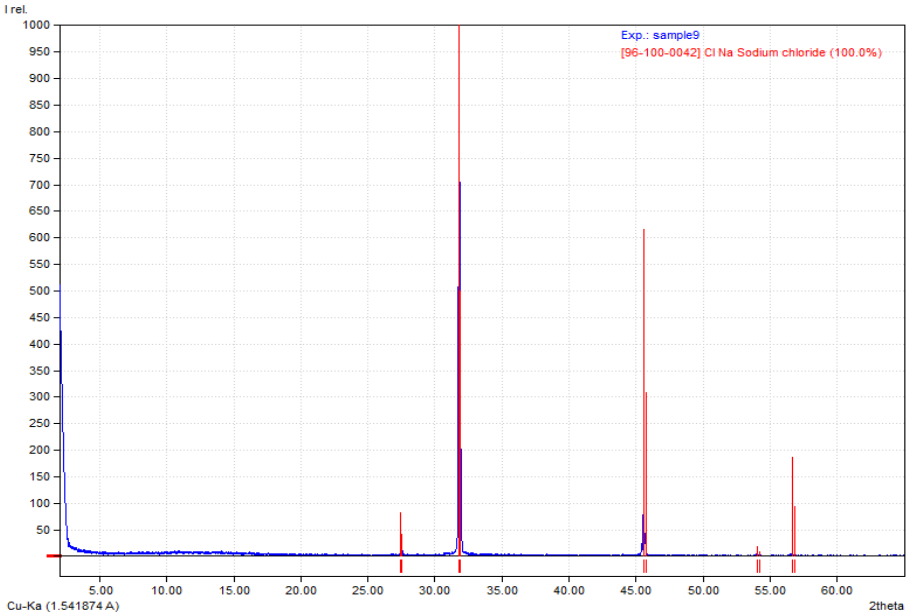

Figure 31: XRD analyses of Well 9

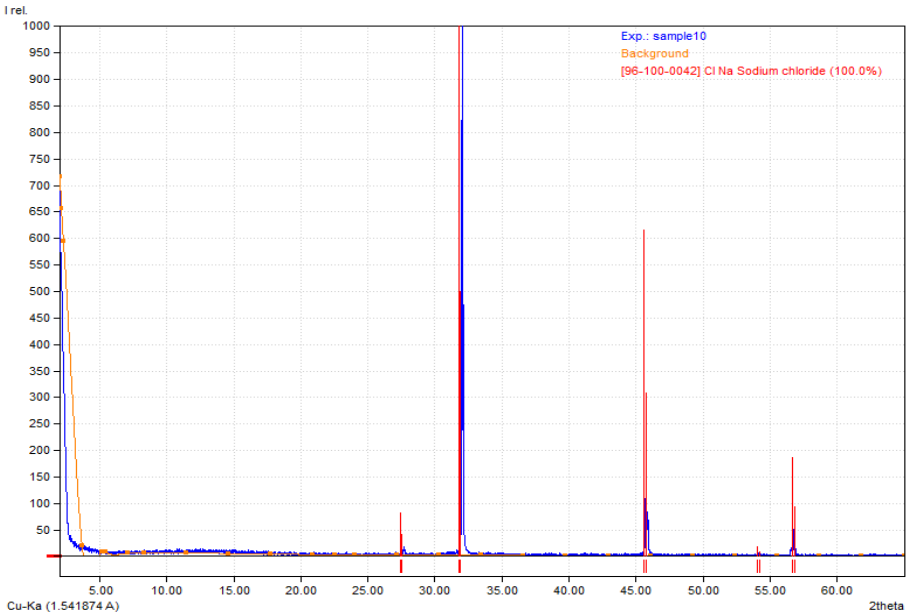

Figure 32: XRD analyses of Well 10

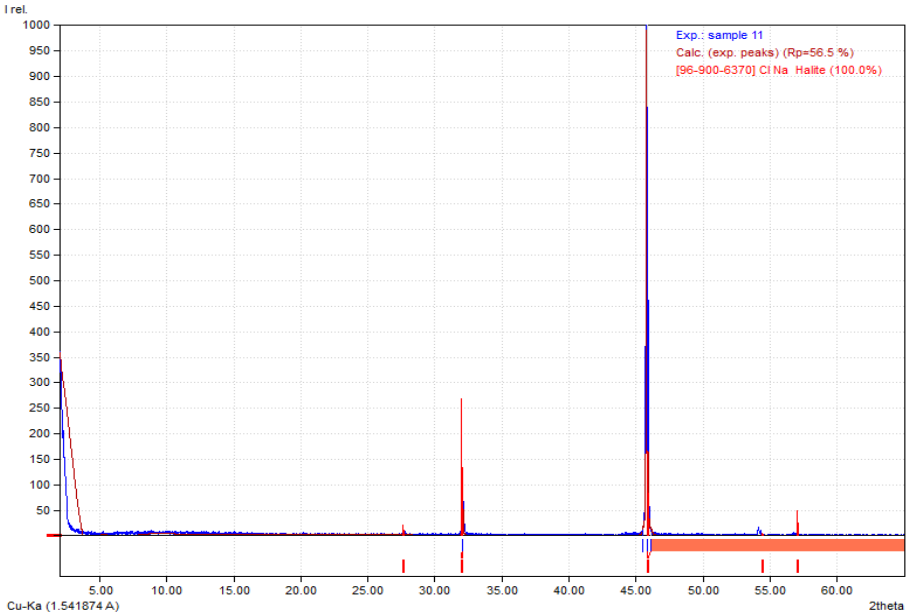

Figure 33: XRD analyses of Well 11

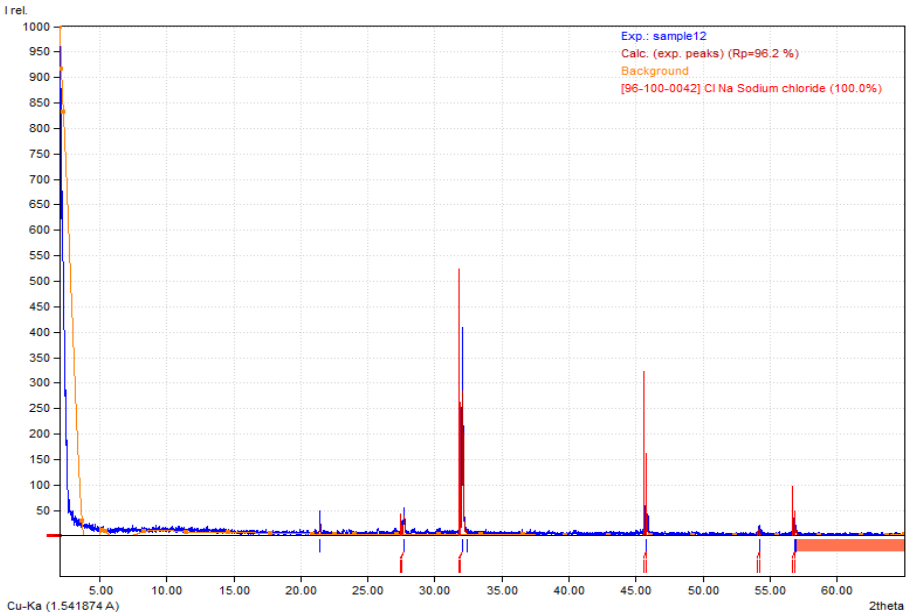

Figure 34: XRD analyses of Well 12

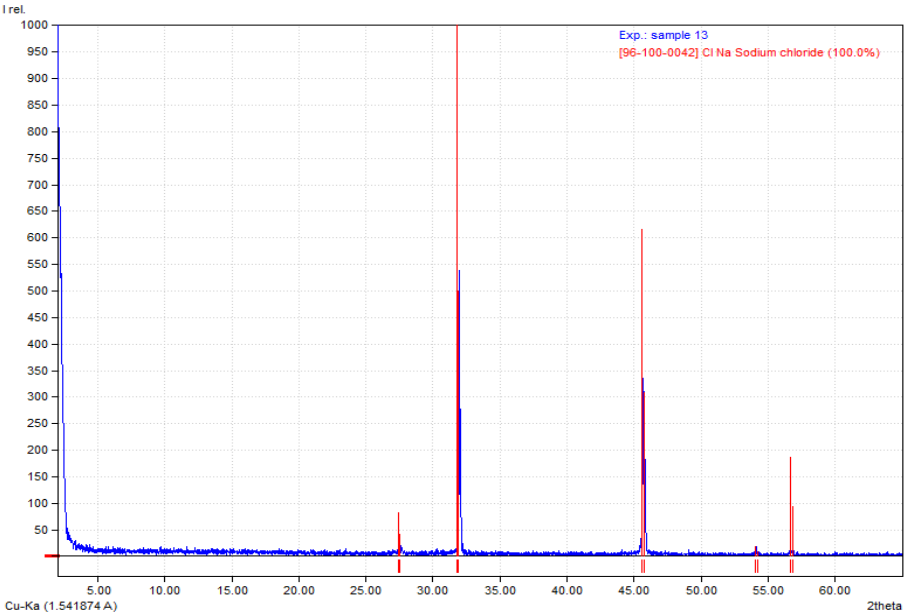

Figure 35: XRD analyses of Well 14

APPENDIX B

TGA RESULTS OF PRODUCED WATER SAMPLES

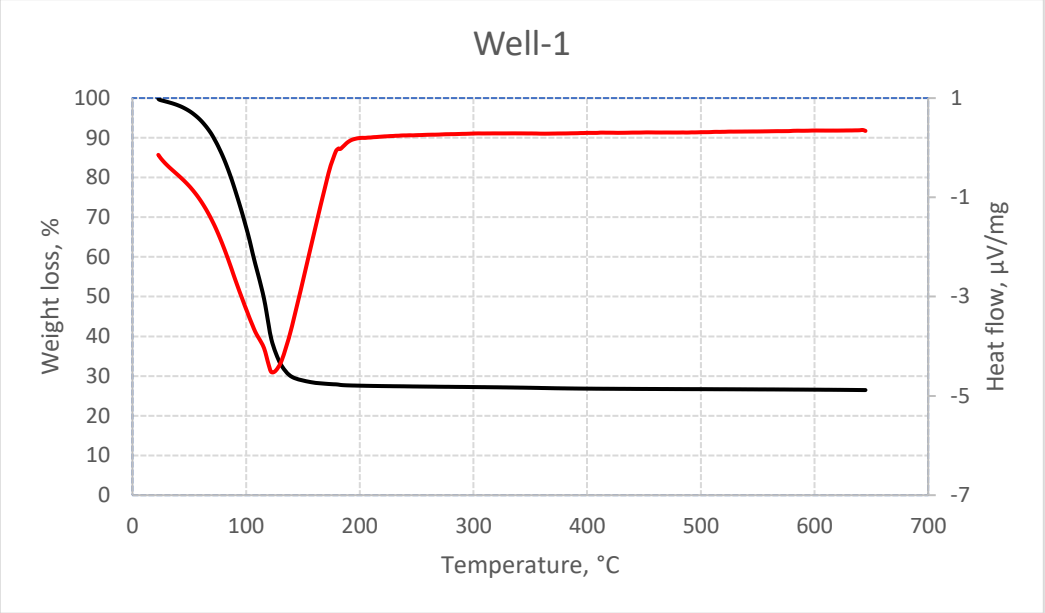

Figure 36: TGA-DSC analyses of a sample from Well 1 (water evaporated at 120ºC)

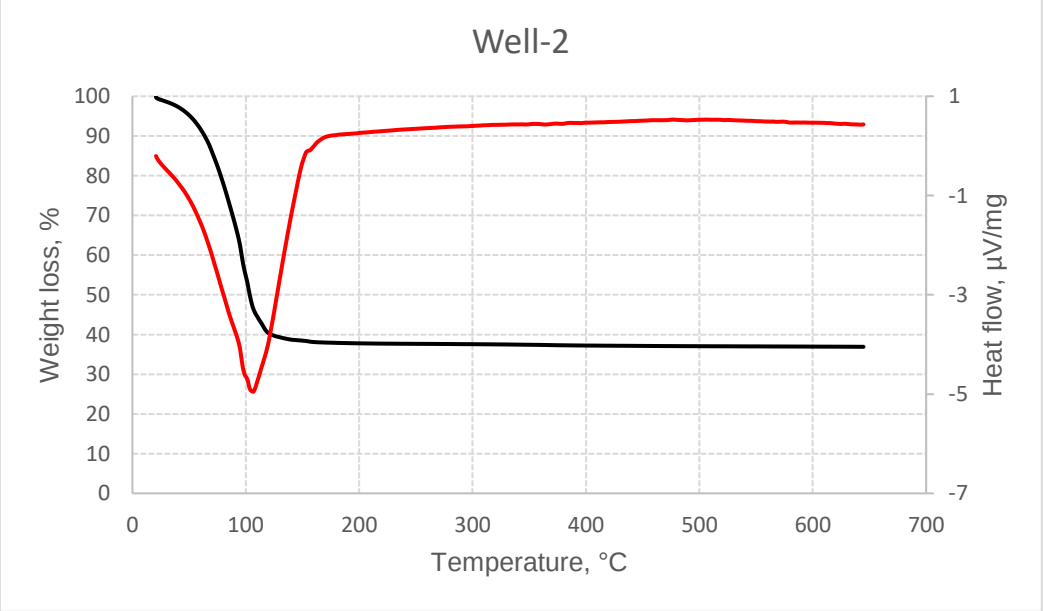

Figure 37: TGA-DSC analyses of a sample from Well 2 (water evaporated at 120ºC)

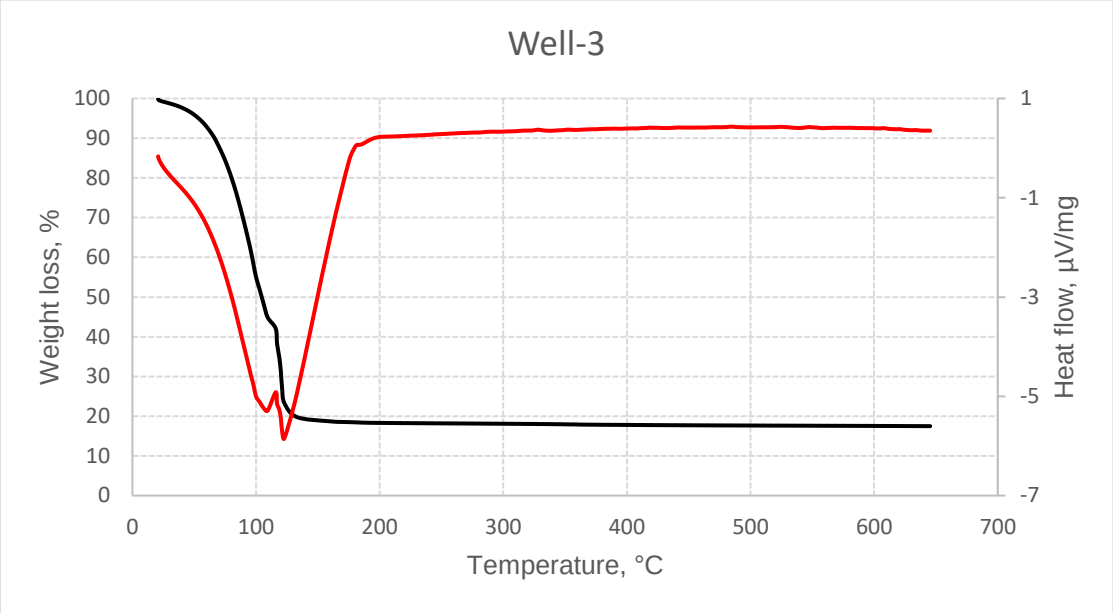

Figure 38: TGA-DSC analyses of a sample from Well 3 (water evaporated at 120ºC)

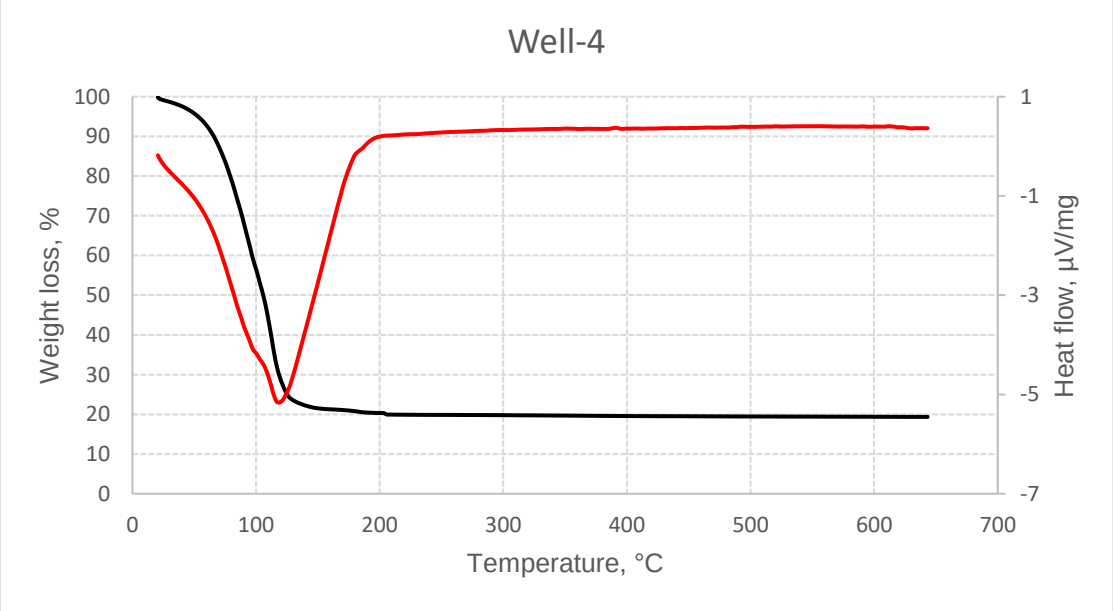

Figure 39: TGA-DSC analyses of a sample from Well 4 (water evaporated at 120ºC)

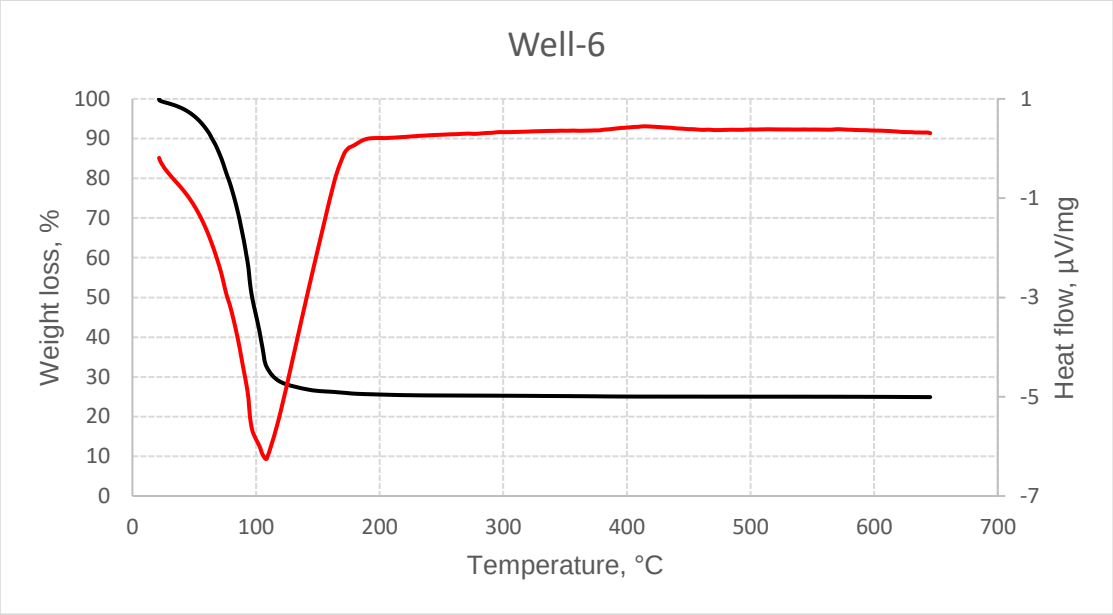

Figure 40: TGA-DSC analyses of a sample from Well 6 (water evaporated at 120ºC)

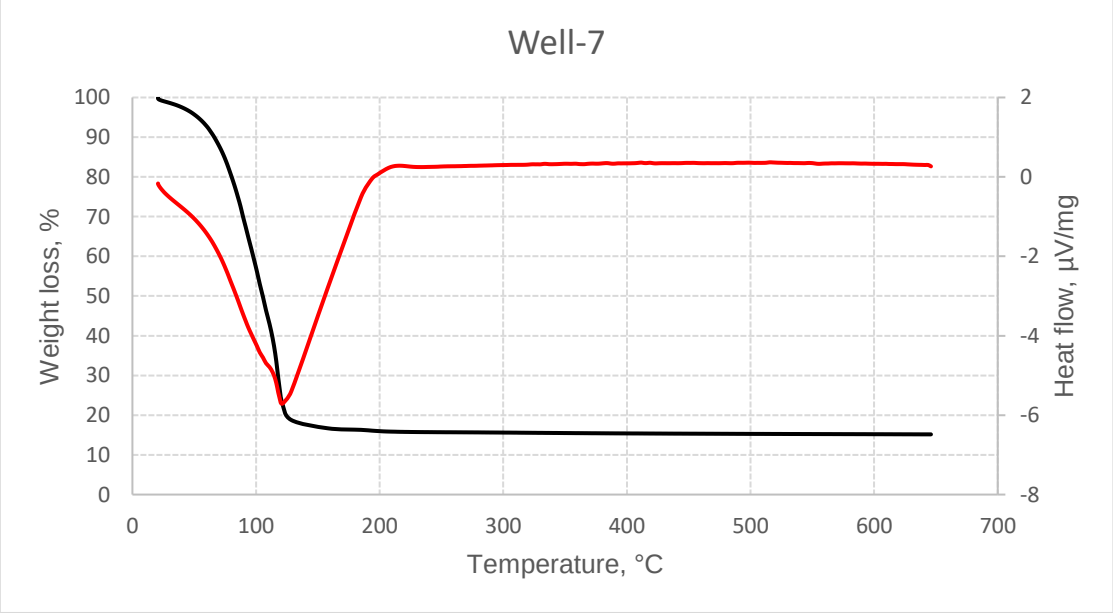

Figure 41: TGA-DSC analyses of a sample from Well 7 (water evaporated at 120ºC)

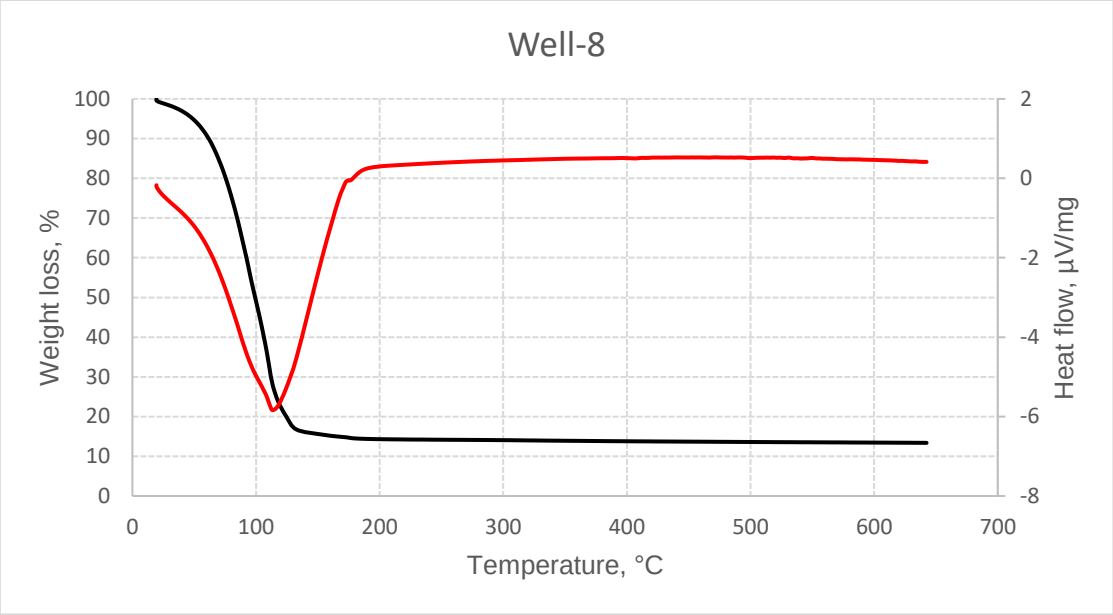

Figure 42: TGA-DSC analyses of a sample from Well 8 (water evaporated at 120ºC)

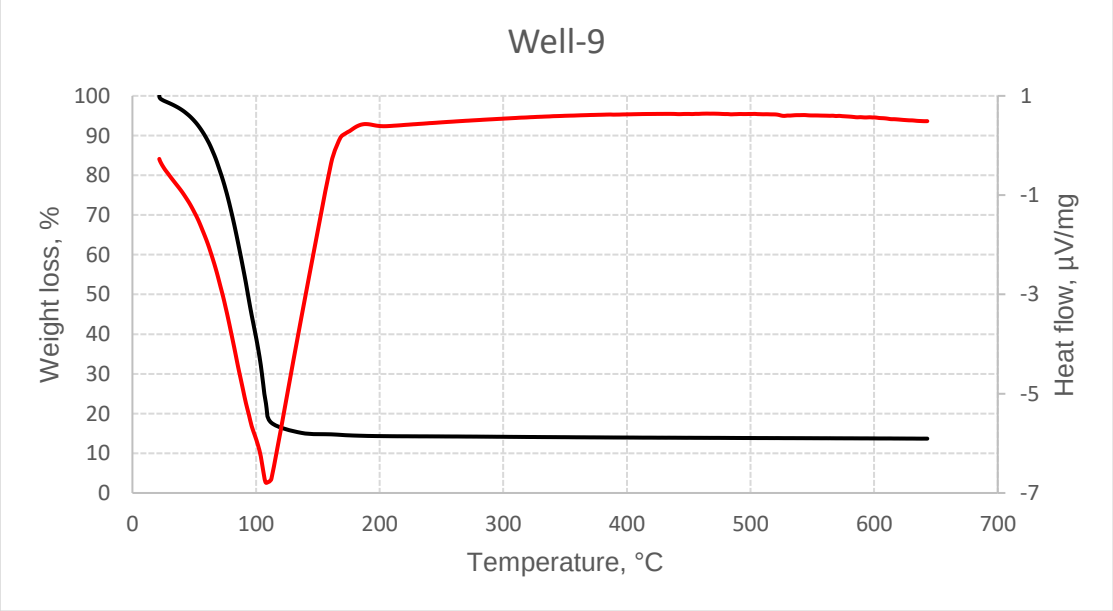

Figure 43: TGA-DSC analyses of a sample from Well 9 (water evaporated at 120ºC)

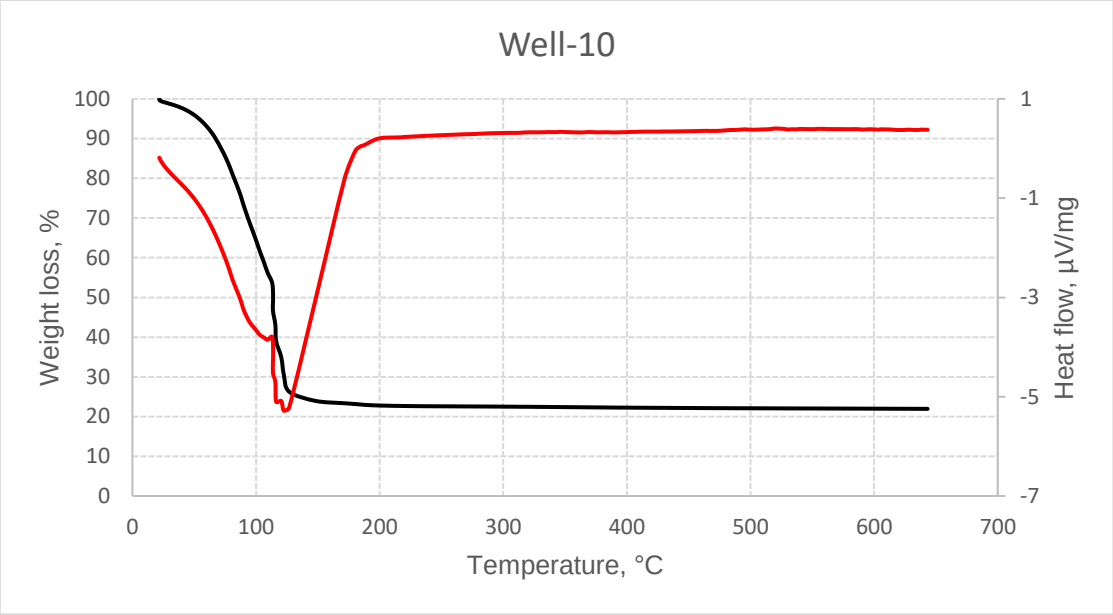

Figure 44: TGA-DSC analyses of a sample from Well 10 (water evaporated at 120ºC)

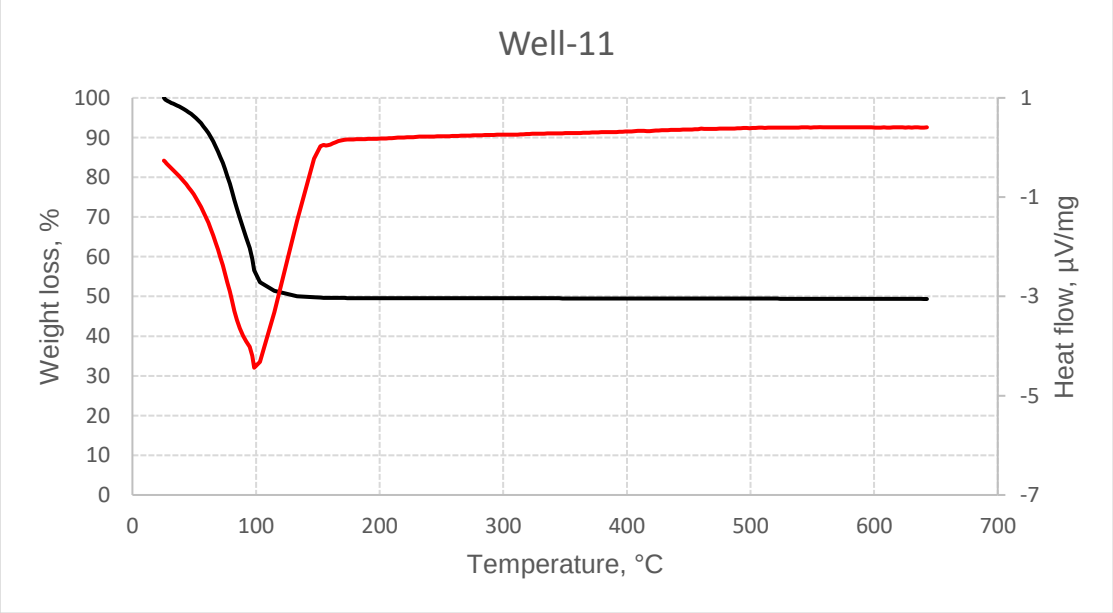

Figure 45: TGA-DSC analyses of a sample from Well 11 (water evaporated at 110ºC)

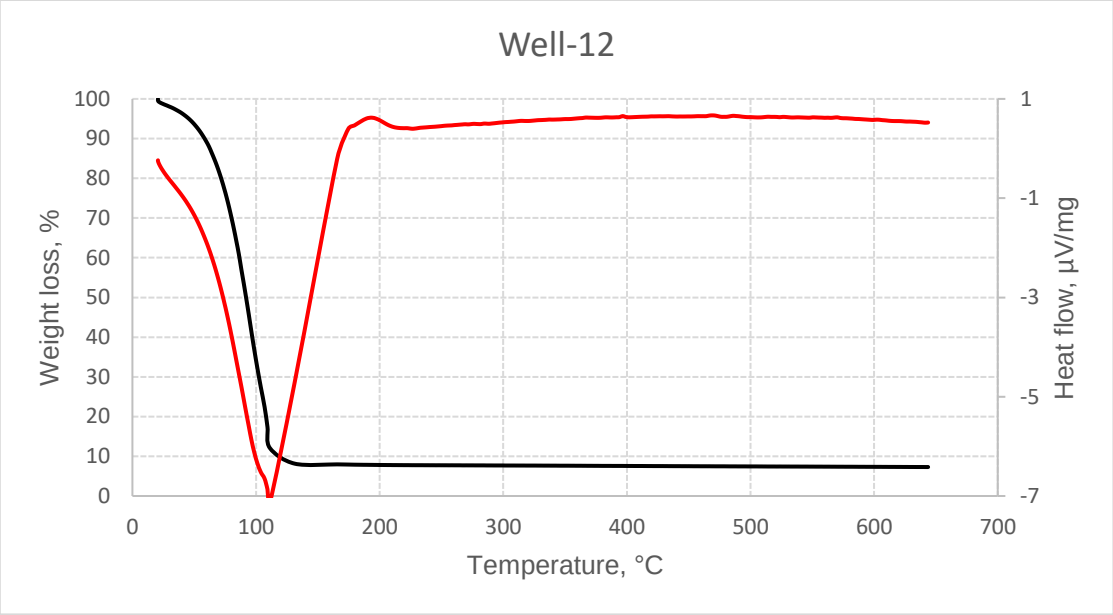

Figure 46: TGA-DSC analyses of a sample from Well 12 (water evaporated at 110ºC)

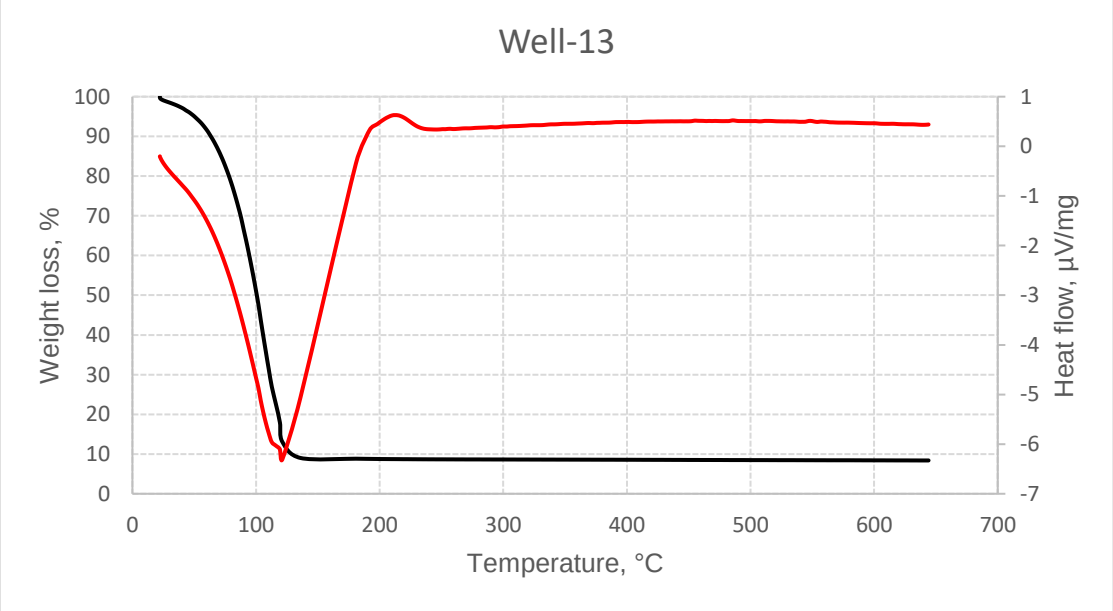

Figure 47: TGA-DSC analyses of a sample from Well 13 (water evaporated at 120ºC)

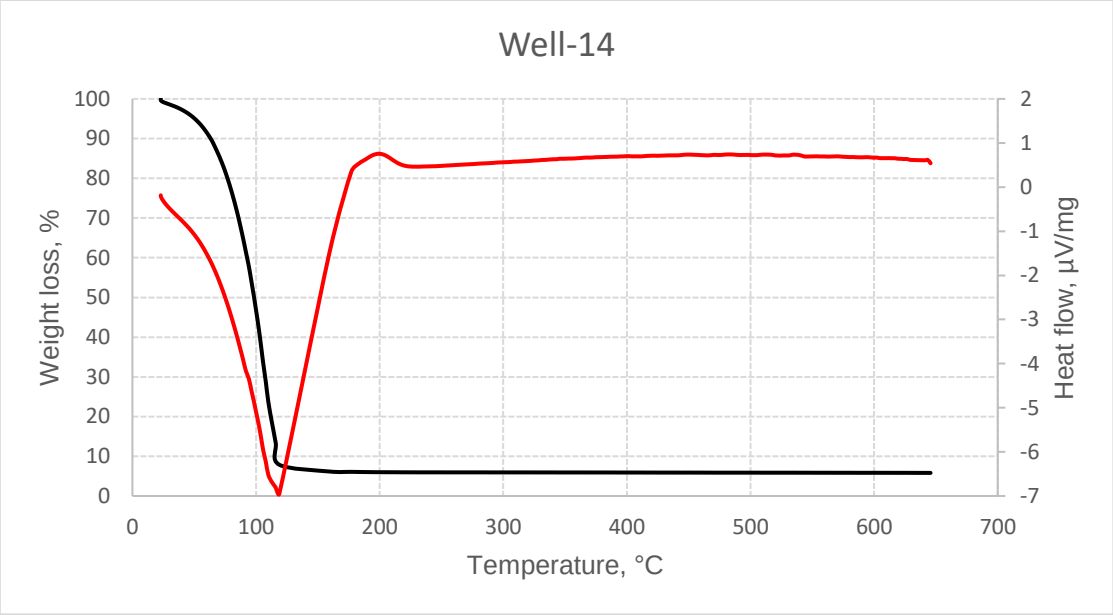

Figure 48: TGA-DSC analyses of a sample from Well 14 (water evaporated at 110ºC)

APPENDIX C

CHARACTERIZATION OF INITIAL WATER SAMPLES

Table 10: TSS, TDS, pH, Zeta potential, and Turbidity values of initial produced water samples of each well

Well number	Turbidity, NTU	TSS, mg/L	pH	ZP, mV	TDS, ppm
1	395	134	7.17	-16	115,000
2	530	162	6.56	-11	116,000
3	167	256	6.87	-14	139,000
4	175	68	6.81	-16	116,000
5	62	31	7.12	-16	118,000
6	265	340	6.92	-11	114,000
7	165	284	6.84	-24	98,500
8	263	245	5.53	-14	115,000
9	195	647	7.11	-22	101,000
10	146	428	6.28	-19	153,000
11	44	18	7.23	-28	58,300
12	49	48	7.48	-27	49,200
13	46	76	7.32	-28	41,500
14	80	20	7.4	-29	42,000

APPENDIX D

ION CONTENT OF PW BY CHROMOTOGRAPHY

Table 11: IC results of produced water samples

	Na	Ca	K	NH4	Mg	Li	Fluoride	Chloride	Bromide	Sulfate
1	43211	4577	741	1612	572	31	33	76155	4445	549
2	53524	5029	825	1497	657	30	ND	111547	819	520
3	66165	2304	768	1574	396	26	11	118786	1601	474
4	50918	5922	488	1139	950	27	ND	110045	866	433
5	41047	7858	1515	843	1384	20	ND	97604	610	394
6	44050	7390	260	724	906	42	ND	107777	1659	472
7	44723	5355	316	890	748	52	46	63720	688	455
8	45217	6659	305	815	834	58	ND	96265	895	386
9	41806	3664	352	971	541	63	44	72220	746	330
10	58991	4115	284	766	689	22	ND	129049	992	739
11	23188	644	399	606	126	19	ND	30978	293	1624
12	22905	1202	351	798	191	18	14	33862	309	1194
13	16444	645	246	260	97	17	27	24129	281	787
14	18435	715	268	276	101	15	16	26476	310	469

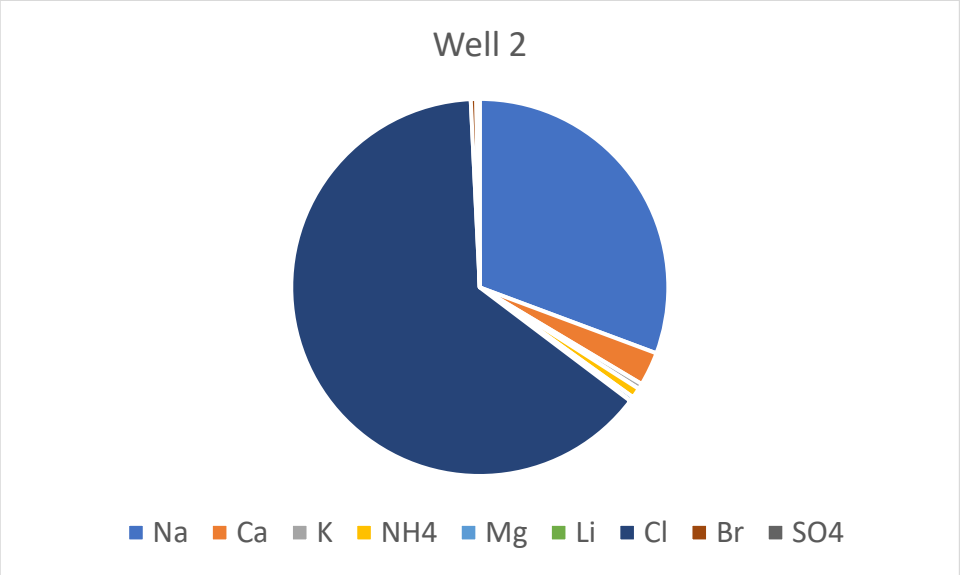

Figure 49: Ion chromatography analysis of Well 2

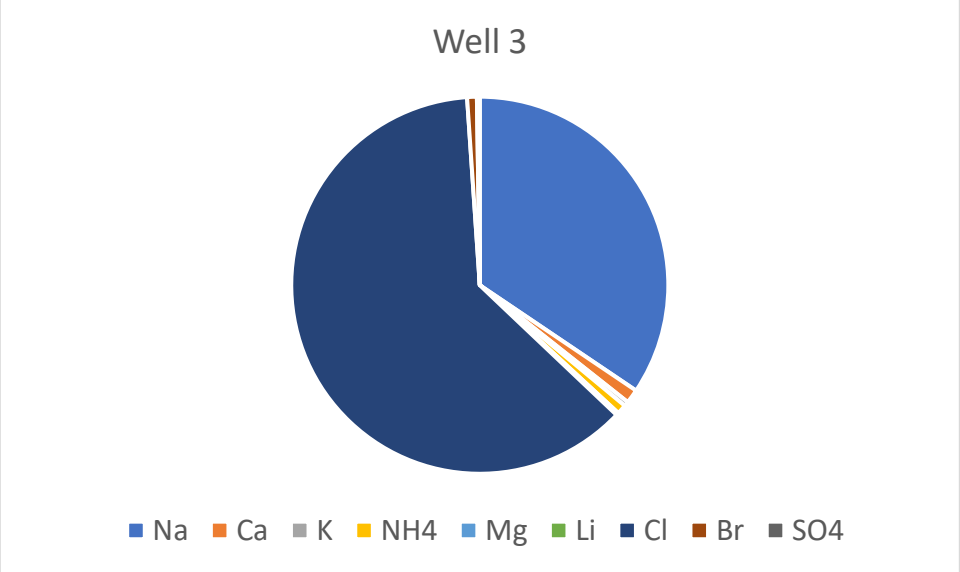

Figure 50: Ion chromatography analysis of Well 3

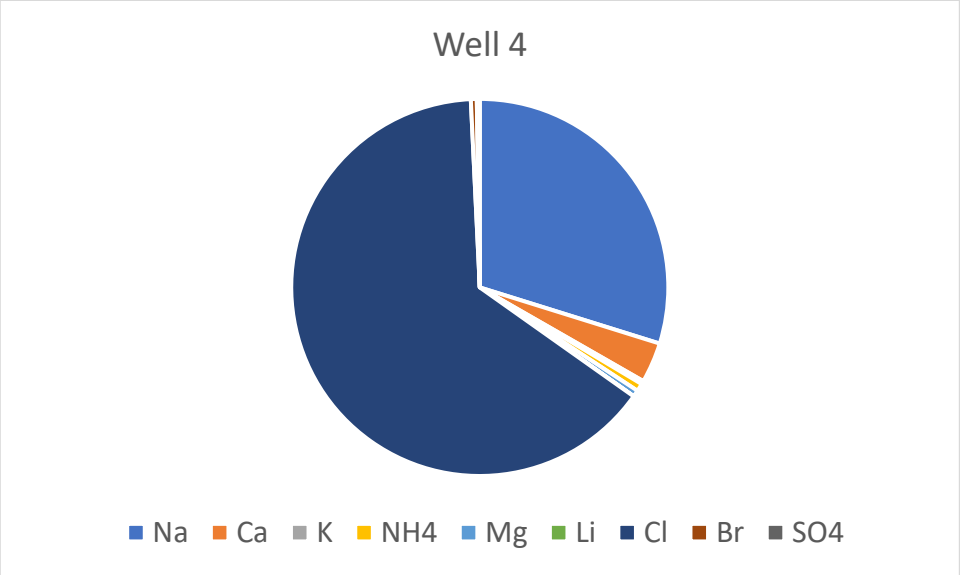

Figure 51: Ion chromatography analysis of Well 4

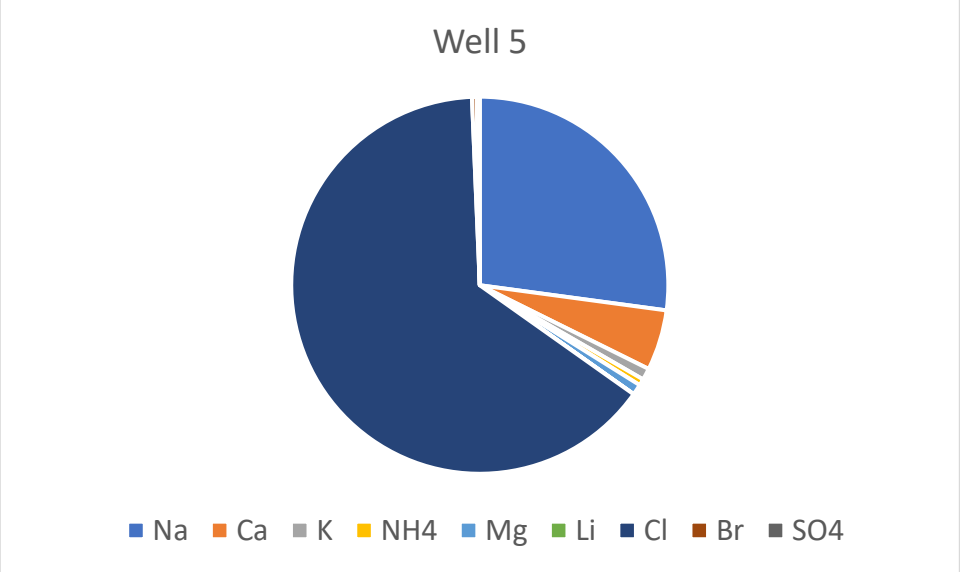

Figure 52: Ion chromatography analysis of Well 5

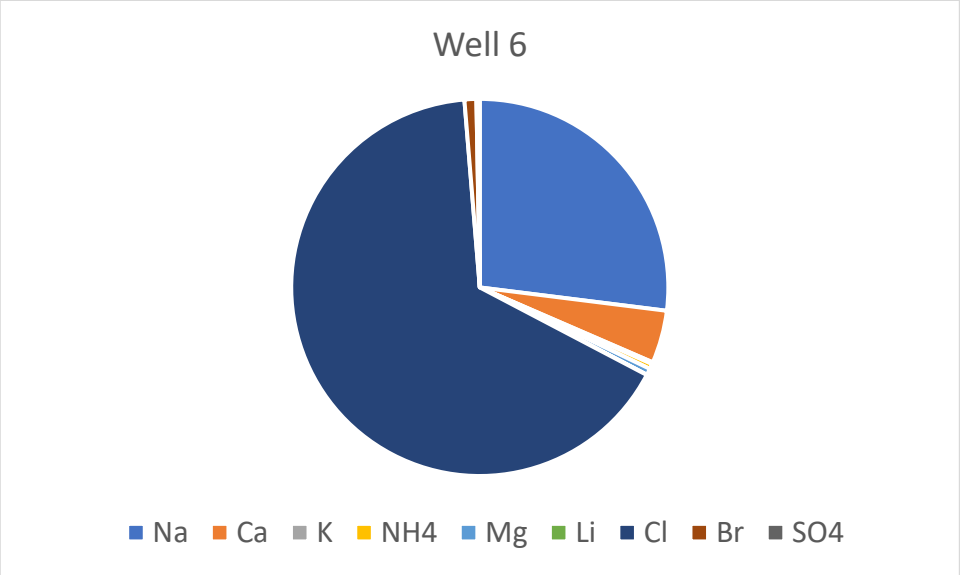

Figure 53: Ion chromatography analysis of Well 6

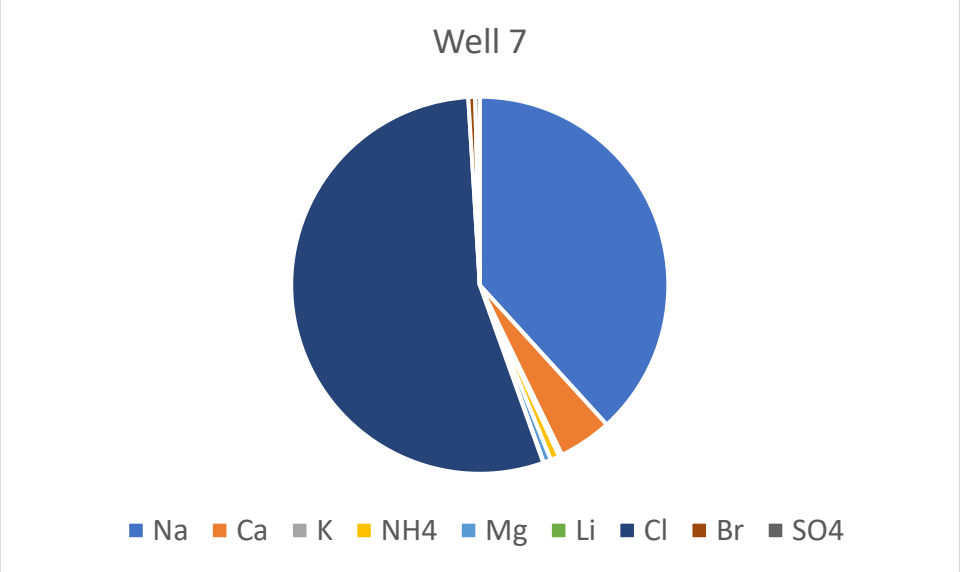

Figure 54: Ion chromatography analysis of Well 7

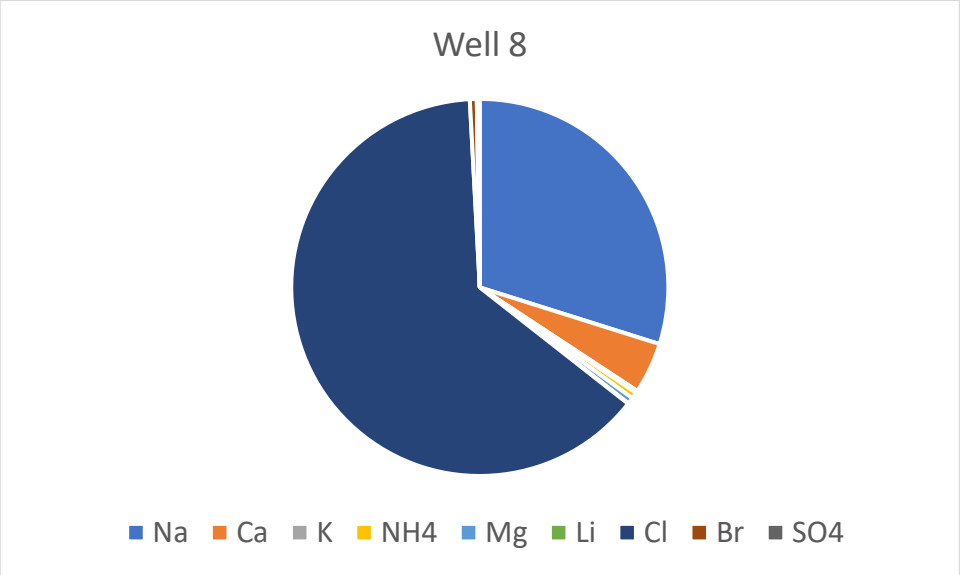

Figure 55: Ion chromatography analysis of Well 8

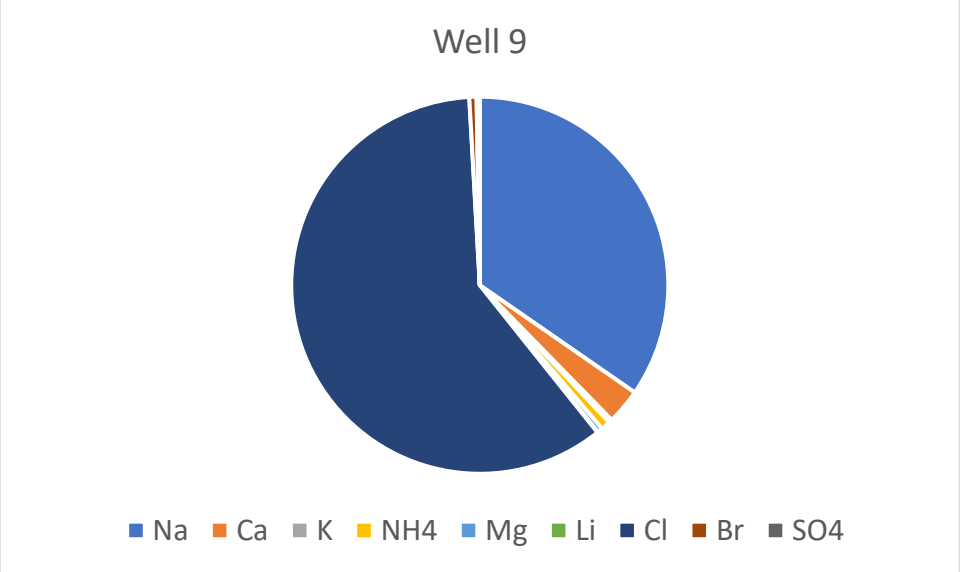

Figure 56: Ion chromatography analysis of Well 9

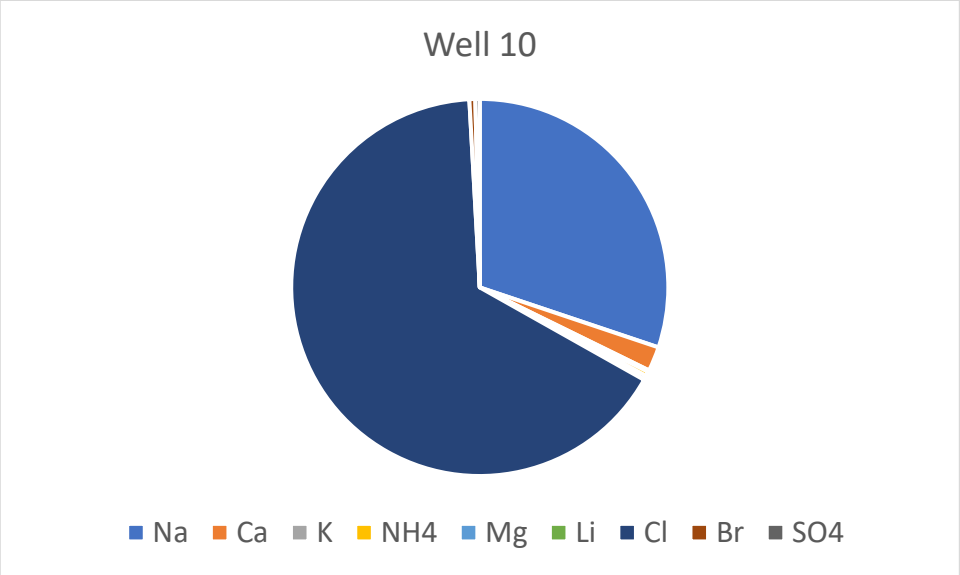

Figure 57: Ion chromatography analysis of Well 10

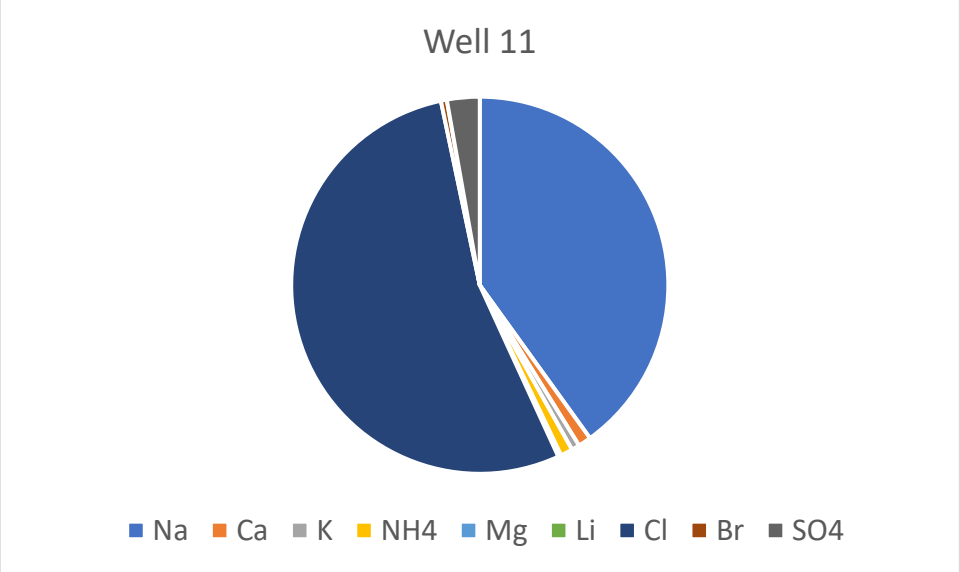

Figure 58: Ion chromatography analysis of Well 11

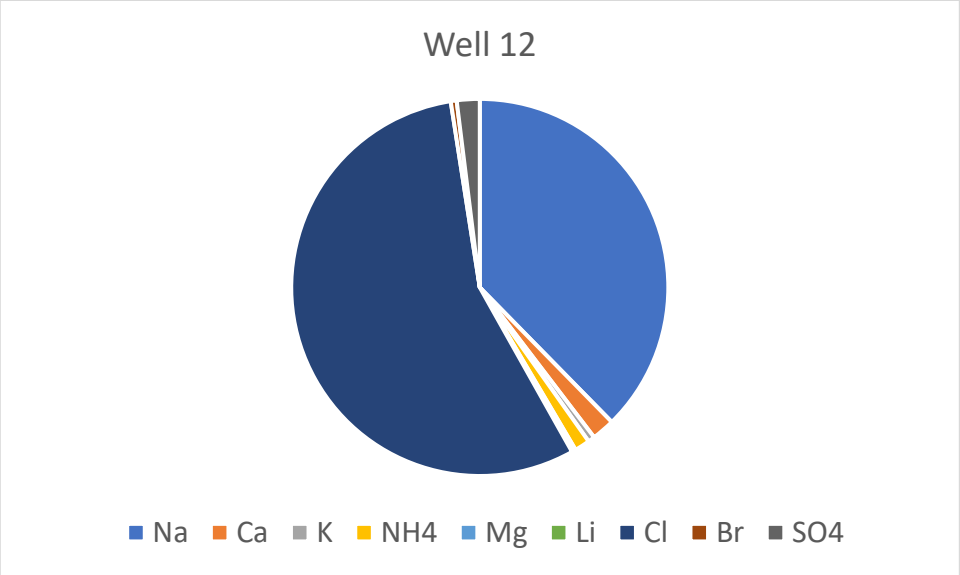

Figure 59: Ion chromatography analysis of Well 12

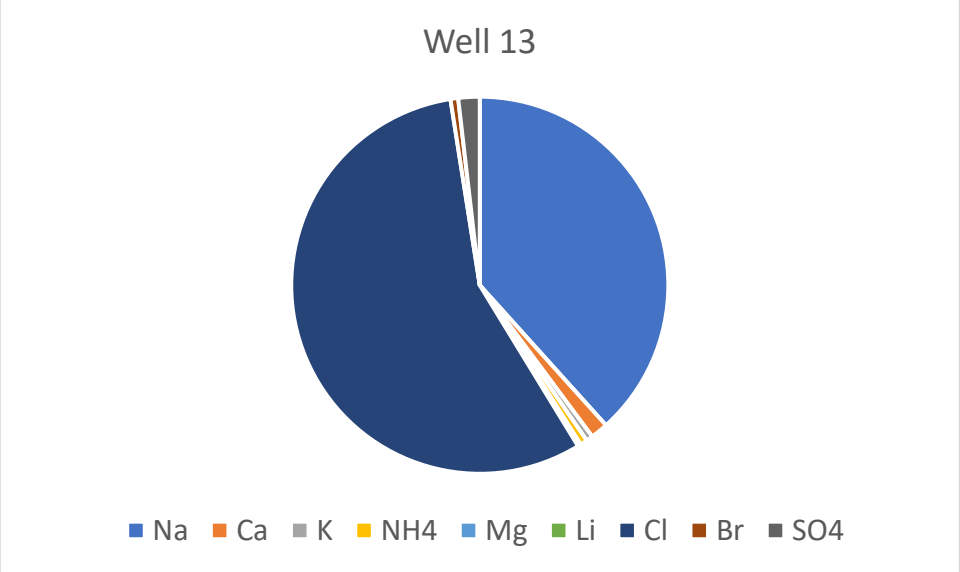

Figure 60: Ion chromatography analysis of Well 13

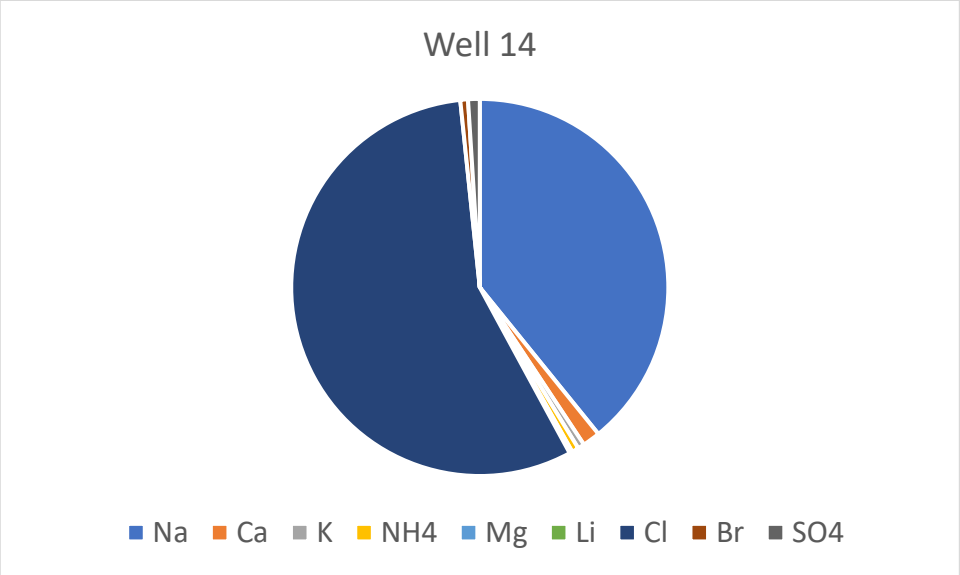

Figure 61: Ion chromatography analysis of Well 14

APPENDIX E

ICP-MS RESULTS OF PRODUCED WATER SAMPLES

Table 12: Ion content of initial PW samples

	Well 1	Well 2	Well 3	Well 4	Well 5	Well 6	Well 7	Well 8	Well 9	Well 10	Well 11	Well 12	Well 13	Well 14
Mo	0.129	0.117	0.147	0.117	0.123	0.115	0.147	0.134	0.120	0.128	0.129	0.117	0.109	0.108
Cd	0.045	0.038	0.037	0.028	0.040	0.036	0.058	0.040	0.027	0.064	0.050	0.051	0.048	0.026
Sb	0.028	0.038	0.022	0.026	0.063	0.020	0.090	0.068	0.062	0.042	0.042	0.032	0.033	0.027
Pb	0.770	0.887	0.732	0.611	1.194	0.591	2.130	1.533	1.138	1.069	0.973	0.850	0.810	0.567
U	0.010	0.015	0.008	0.008	0.026	0.007	0.054	0.044	0.028	0.017	0.021	0.016	0.018	0.015
Al	107	147	68	88	244	80	493	426	251	154	185	149	149	146
Si	198	229	178	167	314	181	451	207	198	171	192	161	189	208
P	0.829	0.958	0.726	0.603	1.065	0.699	1.756	1.313	1.426	3.541	2.750	2.407	2.368	1.640
S	393	559	317	337	693	351	2700	2358	714	924	1896	1401	1342	1130
Ca	7977	8794	4867	10190	12116	12494	11688	12959	7770	9515	4130	3548	3474	2478
Cr	1.463	1.437	1.373	1.341	1.516	1.362	1.931	1.759	1.425	1.524	1.588	1.501	1.444	1.397
Mn	1.441	2.197	1.219	1.424	0.881	1.642	2.949	2.661	2.439	1.568	0.899	0.838	1.068	0.570
Fe	135	71	99	116	86	87	178	91	75	109	99	77	86	107
Co	0.143	0.099	0.092	0.099	0.112	0.074	0.234	0.068	0.227	1.084	0.430	0.501	0.285	0.214
Ni	1.003	1.006	0.887	0.853	1.404	0.877	1.434	0.843	0.882	1.435	1.164	1.085	1.021	0.925
Cu	0.894	0.964	0.533	0.554	1.473	0.486	1.865	1.237	1.288	2.099	1.478	1.336	1.537	0.930
Mg	889	1064	574	1401	1722	1355	1130	1186	806	1213	369	283	229	155
Ti	12.57	19.18	7.68	10.82	33.87	9.39	63.88	54.05	34.01	17.90	20.72	14.19	13.17	12.02
Zn	178	282	360	187	300	146	649	828	758	822	1030	1215	1422	1036
B	103	107	54	58	182	71	170	138	79	54	81	86	113	90
Sr	938	916	1051	1367	962	1234	687	1187	959	613	234	234	263	296

Ba	7.69	6.62	7.36	7.38	9.41	8.50	7.24	28.70	74.44	243	655	1178	1515	1735
K	949	1154	868	685	1852	388	475	403	461	426	553	390	364	318
As	0.018	0.022	0.011	0.017	0.024	0.016	0.052	0.048	0.015	0.022	0.030	0.022	0.016	0.014

Table 13: Ion content of treated PW samples with alum optimal dose

	Well 1	Well 2	Well 3	Well 4	Well 5	Well 6	Well 7	Well 8	Well 9	Well 10	Well 11	Well 12	Well 13	Well 14
Mo	0.10	0.09	0.10	0.11	0.10	0.11	0.10	0.09	0.14	0.15	0.13	0.10	0.12	0.12
Cd	0.02	0.03	0.01	0.07	0.03	0.01	0.01	0.03	0.06	0.06	0.02	0.11	0.05	0.04
Sb	0.05	0.03	0.09	0.10	0.03	0.05	0.03	0.13	0.29	0.09	0.03	0.07	0.12	0.07
Pb	0.79	0.57	0.40	1.12	0.46	0.48	0.45	0.42	0.78	2.05	0.56	1.40	1.21	1.63
U	0.02	0.00	0.01	0.01	0.01	0.01	0.01	0.00	0.01	0.05	0.01	0.00	0.01	0.04
Al	211	57	142	85	96	255	161	58	125	517	115	47	110	396
Si	204	78	151	169	125	219	153	133	168	199	192	132	234	240
P	0.43	0.46	0.27	0.57	0.36	0.58	0.29	0.55	0.99	1.52	0.62	0.51	0.65	0.81
S	608	311	495	413	179	516	675	262	538	2502	1215	673	536	1955
Ca	8401	6509	4325	12689	2263	10367	8091	9809	6874	9460	2168	3194	2586	3838
Cr	1.25	0.96	1.17	1.17	1.12	1.19	1.17	1.03	1.57	1.86	1.49	1.08	1.39	1.54
Mn	1.54	1.71	0.90	1.63	0.32	1.42	2.14	2.10	2.18	1.65	0.52	0.64	0.77	0.77
Fe	37	18	34	20	27	50	120	18	33	82	34	15	22	61

Co	0.05	0.65	0.03	0.13	0.16	0.16	0.03	0.29	0.75	0.07	0.38	0.13	0.17	0.06
Ni	0.70	0.82	0.63	0.92	0.72	0.77	0.63	0.74	1.22	1.54	0.96	0.79	1.09	0.88
Cu	0.77	0.99	0.47	0.50	0.62	0.74	0.54	0.60	1.02	1.62	0.78	0.59	0.65	1.28
Mg	911	801	500	1732	287	1180	1008	1129	825	1072	257	407	264	212
Ti	28.72	5.23	14.35	6.19	9.70	15.82	16.42	5.66	11.62	57.80	10.22	4.32	7.89	50.04
Zn	18.60	18.77	25.65	29.54	23.10	19.14	19.03	23.19	34.65	30.91	20.30	26.83	27.34	9.51
B	133	60	58	68	27	72	72	57	69	102	66	77	108	144
Sr	963	713	962	1691	176	1018	702	1199	977	424	179	361	279	237
Ba	7.94	5.39	6.94	9.27	4.69	9.10	5.81	9.24	8.79	6.38	4.68	3.11	4.49	4.95
K	1045	871	877	843	255	362	423	388	531	453	530	437	381	359
As	0.01	0.01	0.03	0.03	0.01	0.01	0.01	0.03	0.02	0.04	0.01	0.01	0.02	0.04

Table 14: Ion content of treated PW samples with ferric sulfate optimal dose

	Well 1	Well 2	Well 3	Well 4	Well 5	Well 6	Well 7	Well 8	Well 9	Well 10	Well 11	Well 12	Well 13	Well 14
Mo	0.14	0.13	0.10	0.09	0.12	0.11	0.10	0.11	0.10	0.10	0.11	0.10	0.14	0.12
Cd	0.04	0.02	0.02	0.02	0.03	0.05	0.05	0.05	0.07	0.06	0.05	0.03	0.03	0.07
Sb	0.10	0.05	0.03	0.02	0.04	0.06	0.06	0.03	0.04	0.03	0.03	0.03	0.02	0.03
Pb	2.31	0.88	0.56	0.51	0.74	2.52	1.39	0.68	1.24	1.06	1.12	0.62	0.48	0.99
U	0.06	0.02	0.01	0.01	0.01	0.04	0.02	0.01	0.01	0.01	0.01	0.01	0.01	0.01
Al	553	215	96	70	149	439	213	92	133	89	122	96	70	102
Si	326	197	161	126	182	247	202	185	170	116	135	135	188	159
P	1.41	0.64	0.38	0.45	0.80	0.97	0.66	0.63	0.86	0.61	1.60	0.58	0.60	1.19
S	2915	769	285	347	437	1016	788	253	536	597	1246	738	863	475
Ca	11632	7844	4384	8636	11001	12742	9811	8312	6468	6899	1976	2026	2111	2370
Cr	1.86	1.43	1.14	0.99	1.43	1.27	1.25	1.31	1.24	1.22	1.17	1.17	1.39	1.28
Mn	2.15	2.07	0.73	1.11	0.74	2.06	2.65	1.84	2.08	1.08	0.55	0.47	0.73	0.62
Fe	92.13	39.11	32.48	25.38	32.11	139.11	150.81	27.22	32.27	36.56	52.61	37.69	51.93	32.86
Co	0.17	0.11	0.09	0.18	0.13	0.08	0.08	0.21	0.19	0.13	0.44	0.27	0.16	0.47
Ni	0.91	0.76	0.67	0.66	0.94	0.92	0.98	0.89	0.97	0.91	0.91	0.79	0.92	1.14
Cu	1.93	0.92	0.63	0.57	0.99	1.81	1.18	0.72	0.87	0.67	1.36	0.80	0.67	1.07
Mg	960	877	523	1241	1515	1395	1239	954	785	1021	246	219	223	257
Ti	74.72	28.22	11.17	8.20	18.19	53.86	29.70	10.27	15.30	10.17	14.57	10.95	7.07	11.04
Zn	131	106	105	71	159	94	66	166	144	126	62	60	22	186
B	202	95	53	47	138	103	88	59	69	42	58	73	142	95
Sr	902	807	976	1140	840	1149	831	1037	868	499	165	170	308	339
Ba	10.35	6.44	7.93	6.96	8.94	17.89	8.56	9.25	7.73	4.51	3.64	3.32	3.16	5.91
K	1120	991	864	532	1703	423	479	363	583	378	406	356	432	348
As	0.06	0.02	0.01	0.00	0.03	0.04	0.02	0.03	0.03	0.01	0.01	0.01	0.01	0.01

Table 15: Ion content of treated PW samples with polyamine

	W-1 (Alum)	W-6 (Alum)	W-7 (Alum)	W-8 (Alum)	W-9 (Alum)	W-10 (Alum)	W-13 (Alum)	W-6 (Iron)	W-7 (Iron)	W-10 (Iron)
Mo	0.14	0.12	0.11	0.11	0.12	0.12	0.11	0.12	0.12	0.13
Cd	0.05	0.02	0.03	0.03	0.03	0.02	0.02	0.03	0.03	0.03
Sb	0.07	0.04	0.04	0.03	0.02	0.02	0.03	0.02	0.05	0.05
Pb	1.74	0.53	0.48	0.42	0.43	0.33	0.39	0.43	0.55	0.52
U	0.04	0.01	0.01	0.01	0.01	0.01	0.01	0.01	0.01	0.02
Al	402	221	124	117	76	127	107	84	118	174
Si	202	185	161	142	146	152	163	147	171	409
P	1.17	0.48	0.96	0.44	0.55	0.95	0.58	0.57	0.92	1.13
S	2097	574	497	325	283	512	516	334	516	604
Ca	9378	10825	6959	7287	5126	6198	1938	9379	6954	6929
Cr	1.76	1.45	1.37	1.31	1.38	1.37	1.35	1.40	1.38	1.48
Mn	1.82	1.47	1.90	1.55	1.57	0.92	0.61	1.25	1.91	1.15
Fe	72.83	55.55	111.78	24.43	32.41	30.26	23.65	58.35	92.20	48.25
Co	0.25	0.11	0.17	0.26	0.15	0.13	0.16	0.21	0.13	0.11
Ni	1.14	0.85	0.80	0.85	0.89	0.93	0.85	0.84	0.86	0.95
Cu	1.81	0.71	0.60	0.73	1.27	0.52	0.66	0.65	0.73	0.58
Mg	794	1225	876	799	614	910	175	1083	869	982
Ti	49.89	24.95	10.36	14.98	8.15	7.06	12.53	10.57	14.67	14.04
Zn	23.91	9.45	69.40	10.64	14.56	10.74	8.43	8.99	70.18	81.96
B	140	76	58	51	51	38	86	62	62	67
Sr	772	1050	582	846	743	451	199	928	568	434
Ba	9.40	8.22	8.86	7.12	7.34	6.07	4.07	8.10	8.60	80.61
K	927.85	357	333	262	341	334	237	264	350	341
As	0.03	0.01	0.01	0.01	0.01	0.01	0.01	0.01	0.02	0.77

Table 16: Ion content of treated PW samples with cationic starch

	W-1 (Alum)	W-6 (Alum)	W-7 (Alum)	W-8 (Alum)	W-9 (Alum)	W-10 (Alum)	W-13 (Alum)	W-6 (Iron)	W-7 (Iron)	W-10 (Iron)
Mo	0.13	0.11	0.12	0.12	0.13	0.14	0.13	0.12	0.12	0.21
Cd	0.03	0.04	0.02	0.02	0.06	0.07	0.05	0.03	0.02	0.04
Sb	0.05	0.02	0.03	0.02	0.03	0.07	0.04	0.06	0.04	0.07
Pb	0.79	0.48	0.46	0.37	0.54	2.10	0.85	0.82	0.44	0.42
U	0.02	0.01	0.01	0.01	0.01	0.04	0.02	0.02	0.01	0.02
Al	223	139	130	118	150	445	185	208	116	161
Si	185	141	141	145	173	167	176	180	154	461
P	1.69	1.53	1.34	1.29	2.43	2.08	1.69	0.92	0.68	1.60
S	614	345	356	303	542	2319	561	890	558	589
Ca	9112	11679	10972	8518	9863	8055	13174	6778	5513	6825
Cr	1.54	1.32	1.36	1.38	1.39	1.72	1.50	1.48	1.47	1.48
Mn	1.52	1.50	1.81	1.81	1.24	1.43	1.70	1.83	0.90	1.10
Fe	44.83	46.21	41.45	32.53	39.77	76.91	81.76	97.30	40.16	44.00
Co	0.20	0.51	0.21	0.15	0.51	0.63	0.95	0.09	0.09	0.10
Ni	1.04	1.01	0.87	0.85	1.23	1.39	1.21	0.91	0.88	0.87
Cu	1.48	0.82	0.71	0.57	1.06	2.76	2.21	0.88	0.58	0.62
Mg	565	971	821	605	960	266	1057	790	778	887
Ti	29.62	7.61	13.50	10.48	8.37	45.28	21.32	29.95	14.52	13.90
Zn	61.33	55.22	56.01	54.72	60.77	54.31	63.92	117.90	66.35	73.50
B	83.16	46.70	52.00	48.95	37.36	110.24	64.60	75.62	41.34	68
Sr	548	804	830	693	451	147	864	507	352	461
Ba	43.21	41.23	44.33	44.55	40.22	37.41	44.91	7.17	6.35	76.00
K	632	231	244	334	334	326	305	339	289	355
As	0.02	0.00	0.01	0.01	0.01	0.04	0.02	0.02	0.01	0.80